Clifford Heather M. (Orcid ID: 0000-0001-5795-1913)

Spaulding Nicole (Orcid ID: 0000-0001-5159-3078)

Kurbatov Andrei, V. (Orcid ID: 0000-0002-9819-9251)

More Alexander, F M (Orcid ID: 0000-0003-1712-8484)

Korotkikh Elena (Orcid ID: 0000-0001-8169-0733)

Chaplin Joyce (Orcid ID: 0000-0001-6370-4310)

McCormick Michael (Orcid ID: 0000-0001-7964-9387)

Mayewski Paul, A. (Orcid ID: 0000-0002-3360-763X)

A 2000 Year Saharan Dust Event Proxy Record from an Ice Core in the European Alps

Heather M. Clifford[1], Nicole E. Spaulding[1], Andrei V. Kurbatov[1,2], Alexander More[1,3], Elena V. Korotkikh[1], Sharon B. Sneed[1], Mike Handley[1], Kirk A. Maasch[1,2], Christopher Loveluck[4], Joyce Chaplin[5], Michael McCormick[3], and Paul A. Mayewski[1,2]

[1]Climate Change Institute, University of Maine, Orono, ME, United States

[2]School of Earth and Climate Sciences, University of Maine, Orono, ME, United States

[3]Initiative for the Science of the Human Past, Harvard University, Cambridge, MA United States

[4]Department of Archaeology, University Park, School of Humanities, University of Nottingham, Nottingham, UK

[5]Department of History, Harvard University, Cambridge, MA, United States

Corresponding author: Heather Clifford (heather.clifford@maine.edu)

Key Points:

- A well-dated Saharan dust record, spanning 1 -2006 C.E., was produced using chemical analysis of an ice core from the Swiss-Italian Alps

- Use of a novel, non-destructive laser ablation sampling system on ice reveals sub-annual resolution of dust transport to the European Alps

- The tenth century is characterized by continuous, large Saharan dust events, providing evidence for drier conditions in Northern Africa

Abstract

Dust events originating from the Saharan desert have far reaching environmental impacts but the causal mechanism of magnitude and occurrence of Saharan dust events (SDEs) during the pre-instrumental era requires further research, particularly as a potential analog for future climate. Using an ultra-high resolution glacio-chemical record from the 2013 Colle Gnifetti (CG) ice core drilled in the Swiss-Italian Alps we reconstructed a 2000 year-long summer Saharan dust record. We analyzed both modern (1780-2006) and pre-modern Common Era (C.E.) major and trace element records to determine air mass source regions to the Colle Gnifetti glacier and assess similarities to modern and reconstructed climate trends in the Northern Hemisphere. This new pSDE (proxy SDE) reconstruction, produced using measurements from a novel, continuous ultra-high-resolution (120-µm) ice core analysis method (laser ablation-inductively coupled plasma-mass spectrometer or LA-ICP-MS) is comprised of 316,000 data points per element covering the period 1 to 1820 C.E. We found that the CG ice core captures an anomalous increase in Saharan dust transport during the onset of the Medieval Climate Anomaly (870-1000 C.E.) and records other prominent shorter events (C.E., 140-170, 370-450, 1320-1370, and 1910-2000), offering a framework for new insights into the implications of Saharan dust variability.

Plain Language Summary

Plumes of dust from the Saharan desert transported across the Atlantic Ocean and Mediterranean Sea, influence land, ocean and atmospheric systems, yet we know relatively little about how these events varied before the instrumental record. Saharan dust transport can result in flourishing ecosystems, poor air quality and even changes in the frequency of North Atlantic hurricanes. In our study, we develop a summer Saharan dust event record with sub-annual resolution from an ice core drilled in the European Alps, dating back 2000 years. The Saharan dust record shows increased dust transport is caused by a combination of enhanced high-pressure systems over the Mediterranean and drier conditions in Northern Africa, along with other atmospheric influences. Our record indicates the past century has seen an increased amount of Saharan dust transport, comparable to large occurrences over the past 2000 years. Additionally, we discuss implications for using our sub-annually resolved Saharan dust record in concert with historical records to improve interpretations of human-climate interactions.

1 Introduction

Dust transport from the Saharan region to Europe is linked to the state of the climate system (Middleton & Goudie, 2001), yet variability in the intensity of these events is poorly constrained for the past two millennia during which both natural and anthropogenic climate change has occurred. Saharan dust influences terrestrial and ocean biogeochemical ecosystems, human health, and radiative properties of the atmosphere (Goudie & Middleton, 2001). Due to the importance of Saharan dust events (SDEs) to natural systems and human environments, and given the uncertainty of future occurrences of these events in a changing climate, several studies have looked to the past as an analog to understand how SDEs are connected to climate (e.g. Wagenbach, 1989, Angelis & Gaudichet, 1990, Maupeti & Delmas, 1994, Schwikowski et al., 1995, Wagenbach et al., 1995, Schwikowski et al., 1999, Thevenon et al., 2009, Bohleber et al., 2018). To further investigate SDE transport to Europe and their response to changing climates, we present in this paper the longest, continuous, ultra-high-resolution ice core record yet produced reflecting Saharan dust transported to the European Alps. This record was developed using an innovative technique of compiling

continuous measurements from ultra-high resolution (120-µm) LA-ICP-MS technology, applied to the Colle Gnifetti ice core below the firn-ice transition.

Europe and surrounding regions in the Northern Hemisphere experienced several anomalous global climate shifts during the late Holocene including the Medieval Climate Anomaly (MCA; ~ 900-1300 C.E.) (e.g., Lamb, 1965; Bradley et al., 2003; Mann and Jones, 2003; Mann et al., 2009; Berner et al., 2011, Xoplaki et al., 2011), and the following colder era, the Little Ice Age (LIA; ~1350-1900 C.E.) (e.g., Grove 1988; Bradley and Jones 1993; Moberg et al. 2005; Mann et al. 2008). Hypothesized causal mechanisms of these long-term climate events include changes in total solar irradiance (TSI) (Shindell et al., 2001; Renssen et al., 2006), volcanic aerosol loading into the atmosphere (Crowley, 2000; Shindell et al., 2003; Ottera et al., 2010), and ocean circulation (Broecker, 1991; Crowley, 2000). Atmospheric aerosol composition and air mass transport changes provide both a mechanism for and an indicator of transitions in and out of anomalous climate periods and can be measured through chemical fingerprinting of air masses captured in ice cores (Meeker and Mayewski, 2002). Saharan dust deposition reconstructions from 240ka marine sediment records show low latitude dust deposition does not parallel the variability of glacial-interglacial changes seen in mid and high latitude dust emission. Rather, Skonieczny et al. (2019) identified a high correlation to summer insolation on millennial timescales, indicating a significant African monsoon influence on low latitude dust transport. However, relatively little is known about Saharan dust transport during significant climate events of the Common Era such as the LIA and MCA (e.g. Thevenon et al., 2009; Thevenon et al., 2012; Bohleber et al., 2018) and understanding the variability and causality of past climate anomalies can offer essential insights for future climate change (e.g. Antoine & Nobileau, 2006).

Saharan dust transported across the Mediterranean to Central Europe originates from North African sources, predominantly during the spring and summer months, and is typically carried at least 5000 meters above sea level (m a.s.l.; Prospero, 1996; Prospero et al., 2005). Major modern source regions of Saharan dust to Europe include three main areas: Western Sahara, Moroccan Atlas and northern/central Algeria, confirmed through trajectories analyses from northeastern Spain to their area of origin (Avila et al., 1997), also noted in Scheuvens et al. (2013). The transport and deposition of Saharan dust over the Mediterranean in the summer depends on favorable conditions for entrainment and transport of dust above the boundary layer (Gaetani et al., 2014). Past research has shown dust emissions are highest when peak surface heating moves from the Sahel to the central Sahara during the summer months during the northward extension of the Intertropical Convergence Zone (ITCZ), a heavy precipitation band caused by converging northeasterly and southeasterly winds (Engelstaedter et al., 2006). The ITCZ has a southernmost position in the winter months and northernmost in the summer, causing dry convection and convergence, thereby enhancing near surface turbulence and facilitating dust transport (Engelstaedter et al., 2006). Favorable conditions for SDE incursions into Europe during the summer months are influenced by a steepening of the pressure gradient along a strong subtropical high (Azores High), coupled with a northeastward shifting of the Saharan High, located on the northern boundary of the Sahara, into the Mediterranean and a southeast shift in the Icelandic Low (Barkan et al., 2005). Longer transport pathways are also documented from back trajectories reaching out over the North Atlantic prior to transport to Europe (e.g. Schwikowski et al., 1995; Collaud Coen et al., 2004; Sodemann et al., 2006; Thevenon et al., 2012). Although infrequent, Saharan dust has the potential of reaching as far north as the British Isles following an anticyclone over western Europe (Wheeler, 1986; Coudé-Gaussen et al., 1989).

The variability of summer SDEs on an inter-annual to decadal time scale during the modern era has been explained by anthropogenic forcings and ocean-atmospheric

teleconnections such as the North Atlantic Oscillation (NAO), El Nino Southern Oscillation (ENSO), the ITCZ, and the Atlantic multidecadal oscillation (AMO). Human induced soil degradation and increased droughts in the Sahel are linked to increases in dust emissions across the Atlantic (Moulin et al., 2006). However, anthropogenic influences (e.g., desertification, land-use changes, and climate change) on Saharan dust emissions are difficult to resolve precisely due to large natural variability in the arid Saharan region (Moulin et al., 1997; Middleton & Goudie, 2001). For example, we do not yet have the capability to estimate the percentage of anthropogenic dust (Engelstaedter et al., 2006). According to Moulin et al. (1997), enhanced dust transport across the Mediterranean is linked with an increased pressure gradient (r=0.66, p=0.027) associated with the winter NAO index, the difference in normalized winter sea level pressures between Lisbon, Portugal and Stykkisholmur, Iceland (Hurrell, 1995), along with eastward transport over the North Atlantic (r=0.50, p=0.097). Years of high (low) NAO indices are identified by a stronger (weaker) Azores high coupled with a below (above) normal Icelandic Low-pressure system, causing drier (wetter) conditions over southern Europe, the Mediterranean Sea and northern Africa, therefore increasing (decreasing) dust mobilization and transport across the Mediterranean and North Atlantic. Shifts in the ENSO are coupled with changes in lower tropospheric atmospheric circulation over North Africa, causing stronger winds towards the Atlantic Ocean, and therefore enabling SDEs (Prospero & Nees,1986; Prospero & Lamb, 2003; Rodriguez et al., 2015; DeFlorio et al., 2016). A southward displacement in the ITCZ, along with a colder North Atlantic Ocean (negative phase AMO; Wang et al., 2012), prompts a decrease in precipitation and increased surface winds over dust-producing regions in the Southern Sahara leading to amplified SDEs over the North Atlantic, therefore also contributing to Mediterranean transport (Doherty et al., 2012; Doherty et al., 2014). Periods of increased aridity in the Sahara (Middleton, 1985; Littmann, 1991a) and decreased rainfall in the Sahel (Prospero & Lamb, 2003) caused by ocean-atmospheric teleconnections can also play a major role in dust production.

In agreement with Evan et al. (2016), we speculate that any phenomenon that facilitates the transport of dust can lead to an increase in SDEs. Saharan dust, along with other natural and anthropogenic aerosols transported across the Mediterranean are deposited at high elevation glaciers in the European Alps (e.g., Wagenbach, 1989, Angelis & Gaudichet, 1990, Maupeti & Delmas, 1994, Schwikowski et al., 1995, Wagenbach et al., 1995, Schwikowski et al., 1999). Because of the close redundant proximity of the alpine glaciers to population centers, ice core records from these areas capture and preserve unique records of natural and anthropogenic aerosol transport not available through polar ice cores. Ice cores from this region contain the southernmost such records available for the North Atlantic. These records of past dust and sea-salt aerosols offer a history of atmospheric circulation, including strength of wind and pressure systems and changes in air mass sources. Previous ice core studies of aerosols throughout the European Alps include: Col du Dôme, Mont Blanc (Preunkert et al., 2000); Fiescherhorn, Bernese Alps (Schwerzmann et al., 2006); Ortles, Eastern Alps (Gabrielli et al., 2016); and Colle Gnifetti and Colle del Lys in the Monte Rosa region (e.g. Wagenbach et al., 2012, and references therein).

Situated in the heart of the European Alps, Colle Gnifetti (CG) glacier (4500 m a.s.l) stands out as the only non-temperate site where net snow accumulation is low enough to record environmental signals over at least the last two millennia (Bohleber et al., 2018). Previous studies of CG demonstrate it is an ideal site to examine past changes in natural and anthropogenic source aerosols to the European Alps region (e.g., Schotterer et al., 1985; Wagenbach & Geis, 1989; Schwikowski et al., 1995; Lugauer et al., 1998; Thevenon et al., 2009; Meola et al., 2015; More et al., 2017; Bohleber et al., 2018; Loveluck et al., 2018). Due to transport and deposition in relation to meteorological conditions, the primary and most

consistently deposited aerosol transported to CG is Saharan dust (**Figure 1**.; Schotterer et al., 1985). Precise source locations of dust to the Colle Gnifetti region have not been well identified, however back trajectories in concert with chemical tracer measurements by Thevenon et al. (2012) specify regions of Algeria and north-central to north-western part of the Saharan desert (i.e., Morocco, Tunisia, Libya, and Mali), following similar conclusions by Schwikowski et al. (1995). Lugauer et al. (1998) noted the most pronounced aerosol variability captured in modern snow at CG is accumulated during the summer months with some variability recorded during fall and spring and minimal amounts in the winter months.

Building upon the pioneering framework established by Schotterer et al. (1985), Wagenbach & Geis (1989), Schwikowski et al. (1995), and Lugauer et al. (1998) on Saharan dust transport to the European Alps, our research facilitates an advance in understanding aerosol transport to the CG region by utilizing a novel ultra-high-resolution, continuously sampled, two millennia-long, sub-annually dated dust record, from a core collected in 2013 (Bohleber et al., 2018). Previous studies on the 2013 CG ice core have formed a reliable ice core chronology through the combination of annual layer counting paired with previously well-known horizons and newly discovered tephra layers (More et al., 2017; Luongo et al., 2017; Bohleber et al., 2018; Loveluck et al., 2018). Based on annual layer counting and cryptotephra analysis, the CG record goes back to at least 1 C.E. at 61 m (abs) depth with the possibility to extend back even further (Bohleber et al., 2018; Loveluck et al., 2018).

We investigate the recent portion (1780-2006 C.E.) of the 2013 CG ice core record using annually resolved discretely sampled inductively coupled plasma-mass spectrometer (ICP-MS) measurements for signatures of potential air mass sources, then calibrate to modern climate reanalysis data and known Saharan dust events. Using this recent portion of the record as an analog for Saharan dust events, we extend our record back to 1 C.E. using sub-annual (0.02yr) and annually averaged LA-ICP-MS ^{56}Fe, followed by the identification of major dust episodes at 121-μm resolution. The Climate Change Institute's W. M. Keck Laser Ice Facility LA-ICP-MS sampling system was used to collect a total of 316,000 data points for dust element ^{56}Fe over 20-m of core (1 -1820 C.E.). For the LA-ICP-MS ^{56}Fe raw data, an average of 570 data points was collected per year for the first 100 years (1720-1820 C.E.; 3.3m) and an average of 170 data points per year for the entire 20-m of core (1-1820 C.E.). The maximum data points collected in one year for this record is 1,187 in 1818 C.E. This research expands on previous studies that validate LA-ICP-MS technique (Mayewski et al., 2013; Sneed et al., 2015, Haines et al., 2016, Spaulding et al., 2017, More et al., 2017, Bohleber et al., 2018). Applying this novel technique to alpine ice cores allowed us to develop the longest continuous summer Saharan dust record and provide detailed interpretations of past atmospheric conditions on sub-annual to storm-scale event scales.

2 Methods

2.1 Study Area

A 71.8 m deep ice core (N 45.92893, E 7.87627) was recovered in 2013 from the CG glacier located in the Swiss-Italian Alps (**Figure 1**) by a joint ice core drilling expedition from the University of Heidelberg, University of Bern, and the Climate Change Institute (University of Maine) discussed further in Bohleber et al. (2018). Details concerning CG glacier flow, englacial temperature and surface accumulation appear in Alean et al. (1983),

Haeberli et al. (1988), Haeberli and Funk (1991), Lüthi and Funk (2000), Hoelzle et al. (2011), and Konrad et al. (2013).

2.2 High-resolution ice core trace metal and aerosol analysis

Approximately 1,600 discrete samples were collected from meltwater-stream of continuous flow analysis (CFA) at the University of Bern, summarized in Bohleber et al. (2018), then collected clean fractions were also analyzed using the Climate Change Institute's Thermo Electron Element2 ICP-MS instrument to measure concentrations of 26 major and trace elements (Sr, Cd, Cs, Ba, La, Ce, Pr, Pb, Bi, U, As, Li, Al, S, Ca, Ti, V, Cr, Mn, Fe, Co, Na, Mg, Cu, Si, and K) and selected major ions (Cl^-, NO_3^-, SO_4^-) via ion chromatography (IC).

2.3 Continuous ultra-high-resolution laser ablation ice core analysis

Measurements collected from the laser ablation inductively coupled plasma mass spectrometer (LA-ICP-MS) system were compiled to produce an ultra-high-resolution (120-µm per sample) continuously sampled record below the firn ice transition (42-m, 1820 C.E.). Previous studies have also used LA-ICP-MS systems to observe changes in ice (Della Lunga et al., 2014; Della Lunga et al., 2017). In this study, we present only the first ~20-meters below the firn ice transition (42-m to 61-m, 1-1820 C.E). Details regarding method, sample preparation and calibration protocols appear in Spaulding et al. (2017) and Sneed et al. (2015). The same ice sections were previously used in Bohleber et al. (2018) to establish a chronology for the last ~1000 years of the 2013 CG ice core through annual layer counting of a continuous single-element LA-ICP-MS ^{44}Ca record. For the LA-ICP-MS analysis reported here, we applied a new multi-element method to yield a precise investigation of the relative phasing of elements at submillimeter scales (Spaulding et al., 2017). We applied this new multi-element method (Spaulding et al., 2017), to the deepest 30-m of the ice core to create a continuous record for the following elements: ^{56}Fe, ^{27}Al, ^{44}Ca, ^{32}S, and ^{28}Si. An example of data collected from multiple 4-cm runs and 5 concatenated runs in a section appears in **Figure 2**. An explanation of the post-processing of the LA-ICP-MS output data appears in **Text S1**. For each of the 5 elements, we collected close to 500,000 measurements and in total, over 1,500,000 measurements for the 30m of core. As discussed in Sneed et al. (2015) and Spaulding et al. (2017) and further investigated within this study, the resulting intensity values from the dust elements (^{56}Fe, ^{27}Al, and ^{44}Ca) mirror closely their respective elemental concentrations established by traditional ice core sampling. For this study, we disregard ^{32}S, and ^{28}Si measurements as they do not capture as definitively as the dust elements their respective element concentrations compared to traditional ice core sampling from the ICP-MS system. We address gaps in the data >6-cm at: 60.97-61.04-m (7 cm.), 59.44-59.51-m (7-cm), 58.93-59.01 (8-cm), 52.86-52.95-m (9-m), and 58.6-58.74-m (14-cm).

2.4 Time Scale Development

The original CG ice core chronology was established by annual layer counting using a combination of continuous flow analysis (CFA) Ca^{2+} and ultra-high-resolution laser ablation-inductively coupled plasma-mass spectrometer (LA-ICP-MS) single element ^{44}Ca in deeper sections of the core paired with previously well-known horizons such as Saharan dust events (SDEs) and the 1963 bomb radioactivity layers (**Figure S1; Table S1**; Bohleber et al., 2018). Since this work, we found more accurately identified age markers in the original annual layer counting (**Table S1, Figure S1**), including a decrease in lead emissions to natural levels precisely during the Black Death (~1349–1353 C.E.; More et al., 2017) and a large

sulfur/sulfate peak in the 930s, associated with the Icelandic Eldgja eruption (Oppenheimer et al., 2018). The dating uncertainties are adjusted from Bohleber et al. (2018) based on the resolution of ICP-MS measurements at the time marker depth resulting in 5 and 10 years, respectively, for the sudden decrease in lead emissions and the Eldgja sulfur/sulfate peak. In addition, we have refined the original CG time scale with the discovery of a tephra chronological tie point for the 536 C.E. eruption (Loveluck et al., 2018, Hartman et al., 2018). Rhyolitic tephra was identified in a melted ice sample between the depth of 57.67-57.88-m, corresponding to a large peak of S & SO_4^{-2} detected at this depth interval (Loveluck et al., 2018). Based on the geochemical composition of the two tephra particles, Loveluck et al. (2018) concluded that it is similar to the 536 C.E. volcanic event tephra in the NEEM 2011 S1 ice core (Sigl et al., 2015). Based on the preliminary time scale by Boheleber et al. (2018), this depth interval was approximately dated to 470-500 C.E. with an uncertainty of 72 years based on the dating uncertainty. By re-counting annual layers from the Eldgja time marker at 939/940 C.E., the age scale was adjusted by about 50 years at the identified depth interval to 520-550 C.E. with an established age uncertainty of 35 years, accounting for the resolution of the ICP-MS data and the length of the melted core where the tephra was detected. Using our adjusted age scale, the CG record goes back to at least 1 C.E. at 61 m (abs) with an age uncertainty of 75 years (based on the latest adjustment) with the possibility to extend back even further (Bohleber et al., 2018; Loveluck et al., 2018). Future research will be extending the deeper part of the record to the maximum ^{14}C date available (4421–3907 cal yr BP; ~71.73-m) near the bottom of the ice core (Hoffman et al., 2018).

3 Results

3.1 pSDE Record Development

We apply a principal component analysis (PCA) to the entire ice chemistry (co-registered 26 elements, chloride, nitrate, and a sulfate concentrations) dataset (annually-resampled for 1780-2006 C.E.) to reduce dimensionality and find correlations between major and trace elements measured, allowing the identification of significant patterns or relationships within the chemical time series using the sci-kit (v0.20.2) module in Python3.6. The top three resulting principal components (PC) and their total percent variance ($\geq 10\%$) are utilized to distinguish air-mass sources to CG and the European Alps. Anthropogenically emitted pollutants, Pb and Cd, are associated with the third principal component (PC3) capturing 11% of the total variance. PC3 exhibits a notable increase during the 1900s after leaded gasoline was introduced and a sudden drop after the 1980s attributed to lead abatement as previously noted by Schwikowski et al. (2004) in a Mont Blanc firn core. Detailed analysis of Pb from the 2013 CG ice core is discussed in More et al. (2017). Known marine aerosols: Na, Cl and K are the major constituents to the second principal component (PC2), accounting for 14% of the total variance in the record (**Figure 3**). This elemental pattern has been recognized previously by a PCA performed on snow chemistry from the French Alps (Maupetit & Delmas, 1994) and at Fiescherhorn glacier in the Swiss Alps, where K^+ is most highly correlated with the sea-salt elements Na^+ and Cl^- (Schwikowski et al.,1999).

Major crustal elements Fe, Al, Mg, and Ca are associated with PC1 accounting for ~50% of the total variance (**Figure 3**). In agreement with previous studies documenting the elements Fe, Ca, Al and Mg as a part of the chemical signature of Saharan dust, we associate the crustal elements in PC1 with a Saharan origin (e.g., Angelis et al., 1991; Maupetit & Delmas, 1994; Avila et al., 1997; Zhu et al., 1997; Avila et al., 1999; Thevenon et al., 2012; Bohleber et al., 2018). The major dust element Fe has the highest percent variance in PC1

with ~80% variance decomposition (**Table** S2) and has a well-studied presence in the chemical composition of Saharan dust (e.g., Zhu et al., 1997; Goudie & Middleton, 2001; Guieu et al., 2002), therefore we establish it as the prime indicator for SDEs in our study.

We use the ICP-MS Fe concentration measurements for 1780-2006 C.E. to calibrate modern CG SDE (**Figure 4a; Table S3**). We then correlate the ICP-MS Fe concentration to LA-ICP-MS ^{56}Fe intensity measurements for the period of 700-1820 at a 20-yr resolution (gaussian filter, 1σ; r = 0.89, p = <0.01; **Figure S2**). We chose this resolution and time period due to the low resolution of the ICP-MS measurements, below 700 C.E., where the ICP-MS Fe data contains less than 4 measurements per 20-year interval. Using the significant positive correlation to the ICP-MS record and SDEs found in our modern record as support, we created the pSDE (proxy Saharan Dust Event) record using LA-ICP-MS ^{56}Fe intensity measurements for 1 - 1820 C.E. as our primary proxy for Saharan dust transport (**Figure 5a**). Due to the ultra-high-resolution record resulting from the LA-ICP-MS, the difference in number of measurements per year ranges is ~ 170 (mean) to 1,200 (max), thus we have the ability to resample the LA-ICP-MS ^{56}Fe intensity measurements to 0.02 year or 50 data points per year. Weak pSDEs are defined greater than 0.65 percentile above background dust levels (total mean of pSDE record) and below the 0.9 percentile above background; while strong pSDEs are defined as greater than 0.9 percentile above the background dust levels (**Figure 5b**). We assess the results of the SDE record in section 3.2 and the pSDE record in section 3.3.

3.2 Fe-bearing Saharan dust event transport to the European Alps post 1780 C.E.

Figure 4a shows periods of anomalously increased and decreased SDEs from the log-scaled annually resampled SDE record covering the 1780-2006 C.E. period. Notably high concentrations (>0.98 percentile, 47.7 μg/L) occur during the years 1977, 1943, 1937, 1994, and 1984 while 11 of the 12 lowest annual concentrations (<0.05 percentile, 0.75 μg/L) are between the years 1790-1820, also noted as an extremely cold period in Europe (Lamb, 1995). The largest annual peaks (>0.95 percentile, 35 μg/L) interpreted as large SDEs match previously recorded periods of increased dust input to Central Europe, shown in **Table S3**. Among these years of large SDEs, several coincide with the current Sahara/Sahel drought that started in the 1970s, (Prospero & Lamb, 2003). A dust deposition record from northwest Africa, based on a marine-derived grain-size distribution of terrigenous sediments (>10 μm), also shows strong similarities to our record over the past century (Mulitza et al., 2010), apart from the increasing trend since 2000 during where our record is decreasing similar to a wind field controlling most of the North African dust emission variability Northern Africa (Evan et al., 2016).

In order to explore atmospheric circulation systems associated with Saharan dust transported to the European Alps, we describe the relationship of our record to synoptic conditions and factors affecting the North Atlantic/Mediterranean region. Dominant air-mass sources during the summer months to the CG region are Saharan dust-laden winds (**Figure 1**) via northeastward transport across the Mediterranean (Type 1) and less frequent transport northward along the coastline or over the eastern North Atlantic, carried eastward by the westerlies to CG (Type 2), as discussed in Barkan et al. (2005), Varga et al. (2013) and Varga et al. (2014). These two modes of transport are confirmed in back trajectories of Colle Gnifetti by Thevenon et al. (2009) and Schwikowski et al. (1995). Based on the synoptics of dust transport in Barkan et al. (2005) and Varga et al. (2013), Type 1 transport is likely to occur when a high-pressure system is located over NW Africa to central Europe, which is

indicative of a strong Azores high, a northerly shift of cyclones in the North Atlantic and decreased westerly humidity advection to Morocco (Esper et al., 2007). This pattern is also observed in scaled anomaly composites during Feb-June 500 hPa patterns for the 15 driest years in Morocco from 1659-2001 (Esper et al., 2007). MSLP from the 3 largest SDEs in our record after 1979 (1994, 2000, 1984), show a similar pattern over Sardinia caused by a higher than average pressure system presiding over Tunisia and Northern Algeria and into the Mediterranean (**Figure 4b**). From 1870-2006, the annually resolved SDE proxy has a statistically significant correlation (r = 0.66, p = <0.05) to the mean sea level pressure (MSLP) over the Mediterranean (35N-49N;0E-25E) derived from 20CR v2 data set (**Figure 4c**). The 20CR v2 is a reanalysis dataset from NOAA's Earth System's Research Laboratory and Physical Science Division (ESRL and PSD, respectively). Based on their website's description, the analysis uses the Ensemble Filter, described in Compo (2010) and based on Whitaker and Hamill (2002). The dataset runs from late 19th to the 21st century. The dataset is available online through NOAA's ESRL PSD webpage. This correlation along with MSLP anomalies from climate reanalysis data shows Saharan dust is likely to be transported to the European Alps during a stronger Azores High leading to a higher-pressure system residing over NW Africa and the Mediterranean.

3.3. pSDE Variability from 1 to 1820 C.E.

Using the modern record as an analog for climatological conditions favoring periods of notable SDEs, we extend the CG record back to 1 C.E. using our pSDE record. **Figure 5a** demonstrates the 0.02-year (grey) and annual (black) LA-ICP-MS ^{56}Fe (gaussian (2σ), normalized), highlighting the four most significant periods (multi-decadal periods with multiple decades greater than .9 percentile of strong pSDE). We outline the number of strong pSDEs (above .9 percentile above the background dust levels) and weak pSDEs (between 0.65 and 0.9 percentiles above the background) occurring per decade in **Figure 5b,** while thresholds are shown in **Figure 5a**. The four periods include (C.E.): 140-170, 370-450, 870-1000, and 1320-1360, along with the following decades greater than the .9 percentile of strong pSDEs: 570, 60, 670s, 680, 710, 810, 1180, 1200, 1260, 1460, 1520, 1590, 1770 and 1780. The decade with the highest frequency of strong pSDE's occurs in the 430's (193 strong pSDEs), this episode that lasted from 370 to 450 starts with an increase in weak dust events starting in the 400's and strong pSDEs beginning in 410's, then decrease after 430's until the 450's. The longest period of continuous weak and strong pSDE's occurs from 870-1000 C.E., consisting of 871 weak pSDE's and 526 strong SDE's. The decades with the most frequent strong pSDE's during the 870-1000 C.E. period include: 920's (141), 960's (124) and 910's (100). In the 20-year resolution ICP-MS Fe record (**Figure S5**), we detect similar above average periods of SDEs (as compared with the LA-ICP-MS ^{56}Fe record) during 110-170, 360-440, 900-1000 in addition to 1600-1660 (which we do not observe in the pSDE record) and 1880-2000. We additionally observe the increase in pSDEs during the mid-1300s that is not in agreeance with our ICP-MS Fe record.

The variability between the two records might be reflecting methodological differences between the two analyses, therefore the profiles do not mirror each other for every case. The differences include the state of the "ice" when sampling: the ICP-MS measures a melted section of ice, in this case about 1-3 cm resolution while the LA-ICP-MS measures a cleaned surface of solid ice at a much finer resolution. We do not claim they show the same measurements, yet they show similar trends and have a good correlation to each other. This paper is the first time we have used the LA-ICP-MS system to produce a

continuous record longer than a meter, and we believe the general comparison to the ICP-MS data shows satisfactory similarities between the two different measurements.

During three of the four periods with the highest number of weak and strong pSDEs (130-170, 370-450, 870-1000 C.E.), there is a decrease in annual layer thickness (**Figure S3**) that could suggest enhanced snow melt, creating the appearance of abrupt increases and terminations of large pSDE episodes, likely related to accumulation rate or Fe delivery/flux variability. According to Gabbi et al. (2015), high input of Saharan dust during individual years can reduce surface albedo substantially producing a strong influence on snow and ice ablation, while average years of Saharan dust input cause a negligible effect on surface albedo. In addition, enhanced dust concentrations could be a result of re-exposed firn layers with high impurity content due to periods of increased melting (Gabbi et al., 2015)**.** The accumulation rate is variable throughout the core but decreases coevally with three of the largest pSDE episodes. Based on our measurements of Saharan dust variability over the past two millennia, we observe variations of Saharan dust at a decadal scale that do not show a consistent pattern, but that do coincide with the onset of the MCA (Medieval Climate Anomaly), a known major climate transition in European climate.

4 Discussion

4.1 Influences of climate forcings and various large-scale teleconnections on Saharan dust variability

Over the past two millennia, climate variability and changes in atmospheric circulation have been strongly influenced by natural forcings (solar variability and volcanic activity), while more recent changes can be attributed to anthropogenic influences such as land use and greenhouse gas emissions (Mann, 2007). In the case of Saharan dust transport to CG, Thevenon et al. (2009) touch on possible forcing mechanisms (solar, volcanic, anthropogenic) and macro-scale ocean-atmospheric teleconnections (NAO, ENSO, AMO) that have been previously proposed as influences. Here, we attempt to further expand upon the influences of northward SDE transport for multidecadal timescales. To investigate the role of macro-scale ocean-atmospheric teleconnections during the modern period, we correlate the CG SDE record (annual ICP-MS Fe record, 1780-2006 C.E.) to high resolution proxy reconstructions from adjacent regions at 5- and 10-year resolutions (**Table S4; Figure S4)**. We additionally compare our pSDE record to high resolution paleoclimate reconstructions (**Table S5; Figure S5**), with a focus on the onset of the MCA in section 4.2 (**Figure 6**).

4.1.1 Solar and Volcanic Forcings

Statistically significant correlations (**Table S4**) to the Lean et al. (1995) solar irradiance record for 1780-1995 C.E. with our SDE record (**Figure S4**) demonstrates the strong influence of solar forcing on overall trends. Solar forcing is an important influence on European and North Atlantic climate, notably relating to a stronger Azores High (positive NAO), with a lag of 2-4 years (Gray et al. 2013; Gray et al. 2016, Ma et al., 2018). Solar forcing can also influence Northern Hemisphere surface heating (Lean et al., 1995), leading to arid conditions in the Sahara. The relationship between pSDEs and solar activity reconstruction (Steinhilber et al., 2012) from 800-1800 C.E. (**Figure S5**), results in a positive

correlation (**Table S4**) which shows TSI is above average during periods of strong pSDEs, during 140-170, 800-1000 and mid-1300s.

Although limited research has been conducted connecting SDE and volcanic forcing, we speculate on the possibility of volcanic forcing creating suitable conditions for increased SDEs. Volcanic aerosol loading in the stratosphere is associated with positive NAO patterns, cool SST anomalies and a southward shift in the ITCZ, which is in turn associated with increased aridity in Northern Africa, cooling over the North Atlantic, and more frequent and/or more intense ENSO events (Clement et al., 2000; Haug et al., 2001; Moy et al., 2002, Pausata et al., 2015; Birkel et al., 2018). Northern Hemisphere (NH) high latitude eruptions produce changes in atmospheric circulation by creating a blanket of ash particles which block solar radiation thereby causing regional cooling. In the NH summer following an eruption, a weakened African summer monsoon results in decreased precipitation and consequently the flow of the Nile and Niger Rivers (Oman et al., 2006).

While long term impacts of Northern Hemispheric volcanic eruptions on Saharan aridity are under-researched, we observe increases in the average occurrence of pSDEs within the 10 years after the eight largest northern hemisphere eruptions in the Common Era from Sigl et al. (2015; **Figure S6**). Specifically, the increase of pSDE events following the Eldgja (939/940; Oppenheimer et al., 2018) and Laki (1783) events (pSDE, **Figure 5**; SDE, **Figure 4**), respectively, coincide with reduced Nile River flow due to decreased regional precipitation (Oman et al., 2006; Manning et al., 2017). High peaks in Nile River discharge (stronger monsoon intensity) occur during minima in Saharan dust flux records from Western Africa on a multi-millennial timescale over the past 240ka (Skonieczny et al., 2019). Research by Manning et al. (2017) also reveals a decrease in precipitation across the Sahel resulting from a weakened ITCZ due to 20th century eruptions based on CMIP5 modeling results. Additionally, significant correlations result for comparisons of NH Volcanic Forcing (Sigl et al., 2015) with the SDE record for 1780-2000 (**Table S4; Figure S4**) and the pSDE record for 800-1800 C.E. (**Table S5**) suggesting a possible association between NH volcanic forcing and northward Saharan dust transport on multidecadal scales.

4.1.2 North African Winds

The connection between two Saharan dust transport pathways, eastward across the North Atlantic and northward across the Mediterranean (Moulin et al., 1997), is further supported by positive correlations (**Table S4; Figure S4**) between our SDE record and a Saharan dust emission proxy record for westward transport over the Atlantic for 1850-2005 C.E. (Evan et al., 2016). The time series produced by Evan et al. (2016) is derived from NOAA-CIRES 20th Century Reanalysis monthly mean 10-m wind fields accounts for the magnitude and the direction of the wind field controlling most of the North African dust emission variability (**Figure S4**). This suggests that atmospheric phenomena such as ITCZ, NAO, ENSO associated with increased wind across the North Atlantic, may in turn, also cause increased dust transport across the Mediterranean, as previously suggested by Prospero (1996). In addition, Saharan dust laden winds transporting northward are associated warmer temperatures in Europe (Bohleber et al., 2018), further supported by positive correlations

between our SDE record and European temperature (**Table S4, Table S5; Figure S4; Figure S5**) from Luterbacher et al. (2016).

4.1.3 Macro-scale ocean-atmospheric teleconnections

Prolonged periods of wet and dry climate in the Sahel and changes in the African summer monsoon on decadal time scales are influenced by global and regional SST (Giannini et al., 2003). On a regional scale, warmer (cooler) Mediterranean SST increases (decreases) rainfall over Northern Africa as increased moisture is advected southward over the Sahara (Rowell, 2003). On a macro-scale, colder sea surface temperatures (SST) in the North Atlantic are associated with increased dust transport traveling eastward through feedback mechanisms. Wang et al. (2012) state that southward shifts in the ITCZ during periods of cooler North Atlantic SST lead to a decrease in rainfall in the Sahel, followed by an increase in dust production which further cools the North Atlantic Ocean during transport, creating a positive feedback loop. The resulting negative correlation to ERA-Interim reanalysis JJA SST for the 1979-2006 in the North Atlantic, off the coast of NW Africa (**Figure S7**), supports co-variability between North Atlantic SST and northward transport of Saharan dust into Europe. Contrary to previous work, our pSDE and SDE records do not show significant correlations to long-term changes in the North Atlantic sea surface temperature (Mann et al., 2009), rather, two large pSDE intervals (880-950 and 1330-1360 C.E.) match with below average North Atlantic SST (negative AMO).

Sahelian drought has been connected with increased Saharan dust transport across the Atlantic (Prospero & Nees, 1986; Prospero et al., 1995; Prospero ,1996; Prospero & Lamb, 2003), whereas its impact northward across the Mediterranean is less well understood. To determine the influence along the latitude of western Africa (20W-10N), we performed a moving correlation for precipitation rate (mm/day) using 20CRV2c data segmented into four areas from 10N to 35N (**Figure S   8**). Our results show that decreased precipitation in both the Sahel and Sahara play a role in Saharan dust transport northward across the Mediterranean. During the 1880s, a significant negative correlation between precipitation rate at 15-30 N and CG SDE corresponds with an increase in precipitation during a decrease in SDEs. Note the significant positive correlations to Sahel precipitation from 1912-1924. Lastly, the negative correlation with decreased precipitation rate at 25-35 N and increased Saharan dust during 1975 to 2006, corresponds with the Sahelian drought since the 1970s (Prospero & Lamb, 2003). The running average correlations suggest that over the past 30 years or so, northward Saharan dust transport more closely reflects precipitation in the Sahara compared with the Sahel but this co-variability changes over time.

We do not find a statistically significant association between our SDE record and the standard winter NAO reconstructions (Trouet et al., 2009; **Table S4; Figure S4)** during the modern era (1780-2006), reflecting the strength of the summer signal at CG (Lugauer et al., 1998) and the European Alps are in an area variably influenced by the NAO (Casty et al., 2005). However, the SDE record is significantly correlated to the summer NAO (sNAO) reconstruction (Folland et al. 2009; **Table S4**, **Figure S4**). The sNAO is an EOF pattern of observed summertime extratropical North Atlantic MSLP, located farther north than the winter NAO, that exerts a strong influence on European climate and influences summer climate extremes such as flooding, drought and heat stress (Folland et al., 2009). Although the sNAO is well correlated to increased wet weather in the Mediterranean, this pattern has a negative correlation to precipitation in the Sahel, suggesting that a positive sNAO corresponds with Sahelian droughts and a weaker West African Monsoon (Linderholm et al., 2009; Folland et al., 2009). Summer transport of Saharan dust having a weak connection to

the winter NAO index and a stronger correspondence to summer NAO supports previous work (Doherety et al., 2008; DeFlorio et al., 2015). The CG pSDE record therefore suggests that the sNAO has a stronger impact on dust transport compared to the NAO.

Although previous studies suggest North African dust concentrations are associated with ENSO (Prospero & Nees, 1986), our SDE record does not yield a statistically significant correlation (**Table S4; Figure S4**) to the reconstructed ENSO record from Li et al. (2011). ENSO events identified in Prospero & Lamb (2003; 1972–73, 1982–83, 1986–87, 1991–92, and 1997–98), however, occur before major SDEs in our annual post 1780 record, suggesting that although overall trends in ENSO variability disagree, strong winter ENSO events could indirectly affect summer SDE transport through atmospheric teleconnections. The changes associated with strong ENSO circulation patterns can lead to increasing wind speed over tropical Africa and periods of decreased North African/Sahel rainfall (Folland et al., 1986; Janicot et al., 1996). Our data suggests that ENSO variability may have a stronger influence on transport across the North Atlantic compared with the Mediterranean. In relation to ENSO and large-scale atmospheric teleconnections, Thevenon et al. (2009) discovered a potential link between CG SDEs to the South Asian monsoon through a Himalayan ice core (Thompson et al., 2000). Our resulting positive correlations, r-value=0.59, p-value=$7.9*10^{-6}$ (10-year resolution for 1500-1990 C.E.) to the Himalayan ice core dust record (**Figure S9**; Thompson et al., 2000), supports evidence of a connection between northward Saharan dust transport to large-scale teleconnections affecting the South Asian monsoon including the ITCZ.

Based on our analysis, the CG ice core-derived pSDE record is strongly influenced by solar forcing and the summer NAO and is associated with warmer temperatures in Europe. Previous studies and our record provide evidence for a causal climatic relationship between the European Alps, North African hydrology, and North Atlantic SST represented by SDEs. The weak correlations resulting from our initial comparisons to other proxies suggest there is more involved in dust deposition than what previous studies have proposed. Based on comparison to multiple paleoclimate records noted in **Figure S5**, we further suggest that there is not one specific cause of multi-year frequency for large SDEs, but rather multiple influences that create favorable conditions for increased frequency or magnitude of SDEs. Further research beyond our comparisons is necessary to elucidate the complex influences on Saharan dust variability.

4.2 Onset of the Medieval Climate Anomaly

The longest-occurring interval of large Saharan dust events (870-1000 C.E.; **Figure 5, 6**) is coincident with onset of the MCA (900 and 1400 C.E.; e.g., Lamb, 1965; Bradley et al., 2003; Mann and Jones, 2003; Mann et al., 2009; Berner et al., 2011), a period with widespread anomalous droughts, noted in multiple paleoclimate records in Europe, Africa, Asia, and the mid-latitudes of both Americas (e.g. Rein et al., 2004, Pederson et al., 2014; Bhattacharya et al., 2017). On a regional-scale, paleoclimate reconstructions for Africa yield conditions favoring or indicating increased production and transport of dust events during 800-1050 C.E. Most notably, the 3200-year dust deposition record (terrigenous; >10 µm) from the coast of northwest Africa (Mulitza et al., 2010; previously discussed in 3.2) similarly exhibits its largest dust peak (pre-1780) during the mid-900's. Dry conditions between approximately 900-1000 C.E are indicated by an oxygen isotope record of Lake Bosumtwi in Ghana (a proxy for Sahel precipitation; Shanahan et al., 2009) and Moroccan lake level fluctuations (Détriché et al., 2009). Based on high-resolution marine records extracted from the Algerian-Balearic basin (Moreno et al., 2012), higher aeolian African

input is noted in geochemical proxies during the onset of the MCA. and an extremely low frequency of flooding characterizes the period 930 to 1070 in a Nile flood record, further suggesting dry conditions in northern Africa (Hassan et al., 2007). The concurrence of intense drought events in multiple paleoclimate records across the North Atlantic and along the mid-latitudes indicates that these occurrences are linked through ocean-atmosphere teleconnections.

The centennial-long episode of strong pSDEs during the onset of the MCA suggests there was a major change in macro-scale Northern Hemisphere atmospheric teleconnections, favoring sustained drought throughout Africa. Above-average temperatures are documented in the European temperature anomaly data (Luterbacher et al., 2016) while the few NAO Index reconstructions that extend back to at least 800 C.E. suggest a strong Azores High (positive NAO) between 800 and 1200 C.E. (**Figure S5, Figure 6**; e.g. Olsen et al., 2012; Wassenburg et al., 2013; Baker et al., 2015; Faust et al., 2016). The onset of the MCA (870-1000) is indicated as the coldest interval of high-resolution reconstruction documented in diatom-inferred records of August sea surface temperature (Miettinen et al., 2015). In addition, the high resolution AMO reconstruction (Mann et al., 2009) shifts from a colder (more negative) to a warmer (more positive) phase occurring 960 through 1000 (onset of the MCA). North Atlantic SST changes, climatic conditions specified by African hydroclimate records and a positive phase NAO suggest this is a regionally dry period of the MCA. Based on the time period in which this episode of strong pSDEs occurs, we suggest that more frequent input of large pSDEs starting in the 800's could be part of a feedback loop or trigger that caused the MCA in Europe. The abrupt arrival and decline of the episode of strong and weak pSDEs during the onset of the MCA (also seen in ICP-MS record, **Figure S5)** could be indicative of a precursor shift that relayed conditions favorable for pSDEs. The appearance of abruptness and pro-longed strength of pSDEs could also be influenced by changes in surface albedo due to increased dust deposition, yet another indicator that this period is anomalous (Gabbi et al., 2015). Further research on our pSDE record in concert with high resolution paleoclimate proxies is necessary to fully understand the pSDE relationship to the MCA.

Interestingly, this anomalous period of increased large SDEs also coincides with the period generally identified as the economic take-off of France, Germany, Britain and neighboring regions (~900-~1100). Historians and archaeologists have adduced multiple causes and actors (Bartlett 1993, Loveluck 2013), but most agree it started with a medieval Agrarian Revolution in the countryside producing more food to feed more people (White 1966). Historians are now exploring whether improving climate conditions may have contributed to the Agrarian Revolution (Williamson 2013; Brooke 2014, 350-1, 358-64, etc.) The chronological convergence of the SDEs anomaly, some of its salient features, and its geographic scope suggest a link with the climate reorganization in the MCA and, through it, with the take-off of European food production that fueled Europe's demographic and economic expansion. Acknowledging the context of societal changes with exceptional climate-related events is critical to develop more accurate interpretations of increasingly higher resolution paleoclimate data over the Common Era.

4.3 Historic Implications of Ultra-High-Resolution SDEs

Written records that capture evidence of events or inter-annual changes in climate and pollution are highly valuable when used in concert with paleoclimate data, especially when cutting-edge methods of glacio-chemical analysis can reveal environmental signals at a sub-annual scale, as shown in More et al., (2018). This multi-disciplinary approach led to the development of a European lead pollution record for the past two millennia (More et al.,

2017). Using our novel LA-ICP-MS-derived pSDE record, we detect and synthesize environmental signals from the ultra-high-resolution glacio-chemical time series in concert with the written historical records to reveal new multi-disciplinary analysis of paleo environmental signals. For example, the years 1325-1365 C.E. stand out in our record, showing one of the highest concentrations of SDEs (**Figure 5**), while historical records show the 1300s were a time of extreme events beginning with the Great Famine (1315-1317) and ending with the Black Death (1346-1353). Further research should seek to answer whether SDEs further exacerbated a decline in human health by decreasing air quality or if they can be used as indicators for extreme meteorological events leading to human suffering. We focus on the period of 1325-1365 C.E. using our raw 120-μm LA-ICP-MS ^{56}Fe SDE proxy to further examine the possibility of connecting written historical testimonies to dust events analyzed in our record.

The Great Famine (1315-1325 C.E.) predated the occurrence of large pSDEs. Historical evidence shows a period of weather deterioration in this decade—such as torrential rains, floods, mud slides and cold temperatures—which resulted in the death of at least one tenth of the population in northern Europe (Jordan, 1996; Dawson et al., 2007; Jordan, 2010; Campbell, 2010). Our pSDE record is predominantly flat during this period, suggesting Saharan dust events were scarce (with the exception of a moderate event in 1319-1320 C.E.). Based on the patterns described previously, this would suggest a period of increased precipitation, which in fact matches the historical evidence.

Following a small break in the CG glacio-chemical record (**Figure 7**), pSDEs increase in occurrence and magnitude from 1325-1334 C.E.. Historical evidence shows extended droughts (both in summer and winter) in 1323-1337 recorded every year in multiple testimonies, throughout Italy, Northern and Southern France, Belgium, Holland, and Central Europe, with dust recorded in Cologne in 1326 (**Table S6**). Extreme heat events were also recorded in Paris in the winter of 1326-7 and spring/ summer of 1333-4, Central Europe in 1328, the winter of 1331-2 and 1337-8, declining in 1339 with a single heat episode in Southern France. While increased pSDEs recommence from 1340-1350, numerous historical accounts of drought and heat from Germany, Belgium, Austria and Central Europe occur from 1344-1351 (**Table S6**). Blood rain—a phenomenon whereby red, iron-rich Saharan dust falls with rain, appearing similar to blood to contemporaneous observers— was recorded in 1348-1349 C.E. in Germany (**Table S6**).

The shift in occurrence of large SDEs could be explained by a prolonged drought followed by increased winds and atmospheric circulation. Marking the end of the MCA, several Moroccan climate reconstructions covering the mid-1300s suggest a sudden shift from wetter to drier conditions (Esper et al., 2007, Wassenburg et al., 2013, Brahim et al., 2017). For southwestern Morocco, 1350 CE is the driest peak in the entire speleothem record ranging from 831±27 CE to 1935±25 CE (Brahim et al., 2017). Other indicators of a changing climate during this time interval include below average North Atlantic SST (negative AMO) between the interval 1330-1360 C.E. (Mann et al., 2009), coinciding with the first peak in LIA alpine glacier advances from the Great Aletsch glacier located in the Swiss Alps in Europe (Holzhauser et al., 2005). Abrupt changes in atmospheric circulation during the period of 1325-1365 C.E. are reflected in changes in the frequency and magnitude of SDEs in addition to evidence found in historical written records.

5 Conclusions

This study presents the longest continuous, ultra-high-resolution ice core record yet produced, utilized as a proxy for Fe-bearing Saharan dust events via southerly air masses to the European Alps derived from North Africa over the past 2000 years. Environmental signals are well preserved in the CG ice core; thus, the combination of multiple ice core sampling techniques creates a reliable record to interpret the long-term behavior of Saharan dust transport in relation to its occurrence, duration, and magnitude. This study substantially extends in temporal resolution and length of record, the knowledge derived from past ice core studies focused on Saharan dust events transported to CG and the European Alps regions and demonstrates the value of ultra-high-resolution sampling for future ice core records.

Our data suggests the following for SDE variability: 1) interannual to decadal Saharan dust transport to Europe does not vary in a consistent pattern, rather multi-year episodes of frequent, large dust events occur irregularly; 2) covariation between eastward transported North Atlantic and northward transported Mediterranean SDEs during summer months is evident from correlations with North African wind patterns as originally suggested by Evan et al. (2016); 3) multi-decadal Saharan dust transport demonstrates variability similar to key climate transitions in European climate such as the MCA; 4) multi-decadal scale variations in Saharan dust transport allow for further analysis of the influence of multiple ocean-atmosphere teleconnections associated with the North Atlantic including the NAO, AMO, ENSO and the ITCZ; 5) high latitude volcanic activity may result in conditions that are suitable for the amplification of anomalous Saharan dust transport to Europe; and 6) ultra-high-resolution ice core chemistry measurements can be used in concert with historical written records to improve interpretations of human-climate interactions. These findings offer new insights into annual to decadal scale Saharan dust variations during the modern and pre-industrial periods in the European Alps region.

In the past, major dust episodes have been related to Northern African drought accompanied by increased wind speed caused by changes in the pressure-temperature gradient. Based on our study, we predict that warming will result in less frequent but more intense SDEs in the future. In particular, a weaker Azores High (negative NAO) and increased warming in the North Atlantic, due to increased CO_2 emissions, will lead to fewer Saharan dust events across the Mediterranean and subsequently across the North Atlantic. A warming Arctic and increased loss of sea ice will further amplify this effect by weakening the temperature-pressure gradient between the mid and high latitudes, resulting in an even weaker Azores High (negative NAO state) (Magnusdottir et al., 2004). A warming climate will impact the movement of the Intertropical Convergence Zone. On the other hand, intense droughts caused by a reduction in precipitation and increased temperature over northern Africa will lead to increased dust availability and lead potentially to massive periods of dust uplift, causing harm to population centers located in the transport pathways by reducing air quality, as already shown in published case studies of PM10, PM2.5 and other air quality proxies in these areas (de Longueville et al., 2013, Prospero and Mayol-Bracero, 2013, Dimitriou and Kassomenos, 2018).

Acknowledgements

References

Alean, J., Haeberli, W., & Schädler, B. [1983]. Snow accumulation, firn temperature and solar radiation in the area of the Colle Gnifetti core drilling site [Monte Rosa, Swiss Alps]: distribution patterns and interrelationships. Zeitschrift für Gletscherkunde und Glazialgeologie, 19[2], 131-147.

Alexandre, P. [1987]. Le Climat en Europe au Moyen Age: Contribution à l'histoire des variations climatiques de 1000 à 1425, d'après les sources narratives de l'Europe occidentale. Paris: Èd. De l'École des hautes études en sciences sociales.

Angelisi, D. M., & Gaudichet, A. [1991]. Saharan dust deposition over Mont Blanc [French Alps] during the last 30 years. *Tellus B*, *43*[1], 61-75.

Antoine, D., & Nobileau, D. [2006]. Recent increase of Saharan dust transport over the Mediterranean Sea, as revealed from ocean color satellite [SeaWiFS] observations. Journal of Geophysical Research: Atmospheres, 111[D12].

Avila, A., & Penuelas, J. [1999]. Increasing frequency of Saharan rains over northeastern Spain and its ecological consequences. Science of the total environment, 228[2-3], 153-156.

Avila, A., Queralt-Mitjans, I., & Alarcón, M. [1997]. Mineralogical composition of African dust delivered by red rains over northeastern Spain. Journal of Geophysical Research: Atmospheres, 102[D18], 21977-21996.

Baker, A., Hellstrom, J. C., Kelly, B. F., Mariethoz, G., & Trouet, V. [2015]. A composite annual-resolution stalagmite record of North Atlantic climate over the last three millennia. Scientific reports, 5, 10307.

Barkan, J., Alpert, P., Kutiel, H., & Kishcha, P. [2005]. Synoptics of dust transportation days from Africa toward Italy and central Europe. Journal of Geophysical Research: Atmospheres, 110[D7].

Bartlett, Robert. [1993]. *The making of Europe: conquest, colonization, and cultural change, 950-1350*. Princeton, N.J.: Princeton University Press.

Berner, K. S., Koç, N., Godtliebsen, F., & Divine, D. [2011]. Holocene climate variability of the Norwegian Atlantic Current during high and low solar insolation forcing. Paleoceanography and Paleoclimatology, 26[2].

Bhattacharya, T., Chiang, J. C., & Cheng, W. [2017]. Ocean-atmosphere dynamics linked to 800–1050 CE drying in mesoamerica. Quaternary Science Reviews, 169, 263-277.

Birkel, S. D., Mayewski, P. A., Maasch, K. A., Kurbatov, A. V., & Lyon, B. [2018]. Evidence for a volcanic underpinning of the Atlantic multidecadal oscillation. NPJ Climate and Atmospheric Science, 1[1], 24.

Bohleber, Pascal, et al. "Temperature and mineral dust variability recorded in two low-accumulation Alpine ice cores over the last millennium." Climate of the Past 14, no. 1 [2018]: 21.

Bradley, R. S., & Jonest, P. D. [1993]. 'Little Ice Age' summer temperature variations: their nature and relevance to recent global warming trends. The Holocene, 3[4], 367-376.

Bradley, R. S., Hughes, M. K., & Diaz, H. F. [2003]. Climate in medieval time. Science, 302[5644], 404-405.

Brahim, Y. A., Cheng, H., Sifeddine, A., Wassenburg, J. A., Cruz, F. W., Khodri, M., ... & Guyot, J. L. [2017]. Speleothem records decadal to multidecadal hydroclimate variations in southwestern Morocco during the last millennium. *Earth and Planetary Science Letters*, *476*, 1-10.

Broecker, W. S. [1991]. The great ocean conveyor. Oceanography, 4[2], 79-89.

Brooke, John L. [2014]. *Climate change and the course of global history: a rough journey*. Cambridge: Cambridge University Press.

Buisman, J. [1995]. Duizend Jaar Weer, Wind en Water in de Lage Landen. Franeker: Van Wijnen.

Campbell, B.P. [2010] Nature as historical protagonist: environment and society in pre-industrial England. Economic History Review, 63(2), 281-314.

Camuffo, D., & Enzi, S. [1991]. Locust invasions and climatic factors from the Middle Ages to 1800. *Theoretical and Applied Climatology*, *43*[1-2], 43-73.

Casty, C., Wanner, H., Luterbacher, J., Esper, J., & Böhm, R. [2005]. Temperature and precipitation variability in the European Alps since 1500. International Journal of Climatology: A Journal of the Royal Meteorological Society, 25[14], 1855-1880.

Clement, A. C., Seager, R., & Cane, M. A. [2000]. Suppression of El Niño during the mid-Holocene by changes in the Earth's orbit. Paleoceanography, 15[6], 731-737.

Collaud Coen, M., Weingartner, E., Schaub, D., Hueglin, C., Corrigan, C., Henning, S., ... & Baltensperger, U. [2004]. Saharan dust events at the Jungfraujoch: detection by wavelength dependence of the single scattering albedo and first climatology analysis. *Atmospheric Chemistry and Physics*, *4*[11/12], 2465-2480.

Cook, E. R. [2003]. Multi-proxy reconstructions of the North Atlantic Oscillation [NAO] index: A critical review and a new well-verified winter NAO index reconstruction back to AD 1400. Washington DC American Geophysical Union Geophysical Monograph Series, 134, 63-79.

Coudé-Gaussen, G. [1989]. Local, proximal and distal Saharan dusts: characterization and contribution to the sedimentation. In Paleoclimatology and Paleometeorology: Modern and Past Patterns of Global Atmospheric Transport [pp. 339-358]. Springer, Dordrecht.

Crowley, T. J. [2000]. Causes of climate change over the past 1000 years. Science, 289[5477], 270-277.

Dawson, A.G., Hickey, K., Mayewski, P.A., Nesje, A. [2007]. Greenland (GISP2) ice core and historical indicators of complex North Atlantic climate changes during the fourteenth century. The Holocene. 17(4), 427-434.

De Longueville, F., Hountondji, Y. C., Ozer, P., Marticorena, B., Chatenet, B., Henry, S. [2013]. Saharan Dust Impacts on Air Quality: What Are the Potential Health Risks in West Africa? Human and Ecological Risk Assessment, 19(6):1595-1617.

DeFlorio, M. J., Goodwin, I. D., Cayan, D. R., Miller, A. J., Ghan, S. J., Pierce, D. W., ... & Singh, B. [2016]. Interannual modulation of subtropical Atlantic boreal summer dust variability by ENSO. Climate dynamics, 46[1-2], 585-599.

Della Lunga, D., Müller, W., Rasmussen, S. O., Svensson, A., & Vallelonga, P. (2017). Calibrated cryo-cell UV-LA-ICPMS elemental concentrations from the NGRIP ice core reveal abrupt, sub-annual variability in dust across the GI-21.2 interstadial period. The Cryosphere, 11(3), 1297-1309.

Della Lunga, D., Müller, W., Rasmussen, S. O., & Svensson, A. (2014). Location of cation impurities in NGRIP deep ice revealed by cryo-cell UV-laser-ablation ICPMS. Journal of Glaciology, 60(223), 970-988.

Détriché, S., Bréhéret, J. G., Soulié-Märsche, I., Karrat, L., & Macaire, J. J. [2009]. Late Holocene water level fluctuations of Lake Afourgagh [Middle-Atlas Mountains, Morocco] inferred from charophyte remains. Palaeogeography, palaeoclimatology, palaeoecology, 283[3-4], 134-147.

Dimitriou, K. Kassomenos, P. [2018]. Day by day evolution of a vigorous two wave Saharan dust storm – Thermal and air quality impacts. Atmósfera, 31(2): 105-124.

Doherty, O. M., Riemer, N., & Hameed, S. [2008]. Saharan mineral dust transport into the Caribbean: Observed atmospheric controls and trends. Journal of Geophysical Research: Atmospheres, 113[D7].

Doherty, O. M., Riemer, N., & Hameed, S. [2012]. Control of Saharan mineral dust transport to Barbados in winter by the Intertropical Convergence Zone over West Africa. Journal of Geophysical Research: Atmospheres, 117[D19].

Doherty, O. M., Riemer, N., & Hameed, S. [2014]. Role of the convergence zone over West Africa in controlling Saharan mineral dust load and transport in the boreal summer. Tellus B: Chemical and Physical Meteorology, 66[1], 23191.

Engelstaedter, S., Tegen, I., & Washington, R. [2006]. North African dust emissions and transport. Earth-Science Reviews, 79[1-2], 73-100.

Esper, J., Frank, D., Büntgen, U., Verstege, A., Luterbacher, J., & Xoplaki, E. [2007]. Long-term drought severity variations in Morocco. Geophysical Research Letters, 34[17]

Evan, A. T., Flamant, C., Gaetani, M., & Guichard, F. [2016]. The past, present and future of African dust. *Nature*, *531*[7595], 493.

Faust, J. C., Fabian, K., Milzer, G., Giraudeau, J., & Knies, J. [2016]. Norwegian fjord sediments reveal NAO related winter temperature and precipitation changes of the past 2800 years. Earth and Planetary Science Letters, 435, 84-93.

Folland, C. K., Knight, J., Linderholm, H. W., Fereday, D., Ineson, S., & Hurrell, J. W. [2009]. The summer North Atlantic Oscillation: past, present, and future. Journal of Climate, 22[5], 1082-1103.

Folland, C. K., Palmer, T. N., & Parker, D. E. [1986]. Sahel rainfall and worldwide sea temperatures, 1901–85. Nature, 320[6063], 602.

Gabrielli, P., Barbante, C., Bertagna, G., Bertó, M., Binder, D., Carton, A., ... & Davis, M. [2016]. Age of the Mt. Ortles ice cores, the Tyrolean Iceman and glaciation of the highest summit of South Tyrol since the Northern Hemisphere Climatic Optimum. The Cryosphere, 10[6], 2779-2797.

Gaetani, M., & Pasqui, M. [2014]. Synoptic patterns associated with extreme dust events in the Mediterranean Basin. Regional environmental change, 14[5], 1847-1860.

Giannini, A., Saravanan, R., & Chang, P. [2003]. Oceanic forcing of Sahel rainfall on interannual to interdecadal time scales. Science, 302[5647], 1027-1030.

Goudie, A., and Middleton, N. [2006]. Desert Dust in the Global System. Berlin; New York, NY: Springer.

Gray, L. J., Scaife, A. A., Mitchell, D. M., Osprey, S., Ineson, S., Hardiman, S., ... & Kodera, K. [2013]. A lagged response to the 11 year solar cycle in observed winter Atlantic/European weather patterns. Journal of Geophysical Research: Atmospheres, 118[24], 13-405.

Gray, L. J., Woollings, T. J., Andrews, M., & Knight, J. [2016]. Eleven-year solar cycle signal in the NAO and Atlantic/European blocking. Quarterly Journal of the Royal Meteorological Society, 142[698], 1890-1903.

Grove, J. M. [1988]. The Little Ice Age, 498 pp. *Methuen, London*.

Guieu, C., Bozec, Y., Blain, S., Ridame, C., Sarthou, G., & Leblond, N. [2002]. Impact of high Saharan dust inputs on dissolved iron concentrations in the Mediterranean Sea. Geophysical Research Letters, 29[19], 17-1.

Haeberli, W., & Funk, M. [1991]. Borehole temperatures at the Colle Gnifetti core-drilling site [Monte Rosa, Swiss Alps]. Journal of Glaciology, 37[125], 37-46.

Haeberli, W., Schmid, W., & Wagenbach, D. [1988]. On the geometry, flow and age of firn and ice at the Colle Gnifetti, core drilling site [Monte Rosa, Swiss Alps]. Zeitschrift für Gletscherkunde und Glazialgeologie, 24[1], 1-19.

Haeberli, W., Schotterer, U., Wagenbach, D., Schwitter, H. H., & Bortenschlager, S. [1983]. Accumulation characteristics on a cold, high-Alpine firn saddle from a snow-pit study on Colle Gnifetti, Monte Rosa, Swiss Alps. Journal of Glaciology, 29[102], 260-271.

Haines, S. A., Mayewski, P. A., Kurbatov, A. V., Maasch, K. A., Sneed, S. B., Spaulding, N. E., ... & Bohleber, P. D. [2016]. Ultra-high-resolution snapshots of three multi-decadal periods in an Antarctic ice core. Journal of Glaciology, 62[231], 31-36.

Hartman, L., Kurbatov, A., Yates, M., Davies, S., Bohleber, P., McCormick, M., ... & Sneed, S. (2018, April). Microanalysis of Fine Insoluble Particulates from the Colle Gnifetti Ice Core. In EGU General Assembly Conference Abstracts (Vol. 20, p. 11503).

Hassan, F. A. [2007]. Extreme Nile floods and famines in Medieval Egypt [AD 930–1500] and their climatic implications. Quaternary International, 173, 101-112.

Haug, G. H., Hughen, K. A., Sigman, D. M., Peterson, L. C., & Röhl, U. [2001]. Southward migration of the intertropical convergence zone through the Holocene. Science, 293[5533], 1304-1308.

Hoelzle, M., Darms, G., Lüthi, M. P., & Suter, S. [2011]. Evidence of accelerated englacial warming in the Monte Rosa area, Switzerland/Italy. The Cryosphere, 5[1], 231-243.

Hoffmann, H., Preunkert, S., Legrand, M., Leinfelder, D., Bohleber, P., Friedrich, R., & Wagenbach, D. [2018]. A New Sample Preparation System for Micro-14 C Dating of Glacier Ice with a First Application to a High Alpine Ice Core from Colle Gnifetti [Switzerland]. Radiocarbon, 60[2], 517-533.

Holzhauser, H., Magny, M., & Zumbuühl, H. J. [2005]. Glacier and lake-level variations in west-central Europe over the last 3500 years. The Holocene, 15[6], 789-801.

IPCC [2014]. Climate Change 2014: Impacts, Adaptation, and Vulnerability. Part B: Regional Aspects. Contribution of Working Group II to the Fifth Assessment Report of the Intergovernmental Panel on Climate Change [Barros, V.R., C.B. Field, D.J. Dokken, M.D. Mastrandrea, K.J. Mach, T.E. Bilir, M. Chatterjee, K.L. Ebi, Y.O. Estrada, R.C. Genova, B. Girma, E.S. Kissel, A.N. Levy, S. MacCracken, P.R. Mastrandrea, and L.L. White [eds.]]. Cambridge University Press, Cambridge, United Kingdom and New York, NY, USA, 688 pp.

Janicot, S., Moron, V., & Fontaine, B. [1996]. Sahel droughts and ENSO dynamics. Geophysical Research Letters, 23[5], 515-518.

Jordan, W. C. [2010], The Great Famine Revisited. In Bruce, S. D. ed., Ecologies and Economies of Medieval and Early Modern Europe. Boston: Brill.

Jordan, W. C. [1996]. The Great Famine: Northern Europe in the Early Fourteenth Century. Princeton: Princeton University Press.

Konrad, H., Bohleber, P., Wagenbach, D., Vincent, C., & Eisen, O. [2013]. Determining the age distribution of Colle Gnifetti, Monte Rosa, Swiss Alps, by combining ice cores, ground-penetrating radar and a simple flow model. Journal of Glaciology, 59[213], 179-189.

Lamb, H. H. [1965]. The early medieval warm epoch and its sequel. Palaeogeography, Palaeoclimatology, Palaeoecology, 1, 13-37.

Lean, J., Beer, J., & Bradley, R. [1995]. Reconstruction of solar irradiance since 1610: Implications for climate change. Geophysical Research Letters, 22[23], 3195-3198.

Lechleitner, F. A., Breitenbach, S. F., Rehfeld, K., Ridley, H. E., Asmerom, Y., Prufer, K. M., ... & Polyak, V. [2017]. Tropical rainfall over the last two millennia: evidence for a low-latitude hydrologic seesaw. Scientific Reports, 7, 45809.

Li, J., Xie, S. P., Cook, E. R., Huang, G., D'arrigo, R., Liu, F., ... & Zheng, X. T. [2011]. Interdecadal modulation of El Niño amplitude during the past millennium. *Nature climate change*, *1*[2], 114.

Li, J., Xie, S. P., Cook, E. R., Morales, M. S., Christie, D. A., Johnson, N. C., ... & Fang, K. [2013]. El Niño modulations over the past seven centuries. Nature Climate Change, 3[9], 822.

Linderholm, H. W., Folland, C. K., & Walther, A. [2009]. A multicentury perspective on the summer North Atlantic Oscillation [SNAO] and drought in the eastern Atlantic Region. Journal of Quaternary Science: Published for the Quaternary Research Association, 24[5], 415-425.

Littmann, T. [1991]. Rainfall, temperature and dust storm anomalies in the African Sahel. Geographical Journal, 136-160.

Loveluck, C. P., McCormick, M., Spaulding, N. E., Clifford, H., Handley, M. J., Hartman, L., ... & Sneed, S. B. [2018]. Alpine ice-core evidence for the transformation of the European monetary system, AD 640–670. Antiquity, 92[366], 1571-1585.

Loveluck, Christopher. [2013]. *Northwest Europe in the early Middle Ages, c. AD 600-1150: a comparative archaeology*. Cambridge: Cambridge University Press.

Lugauer, M., Baltensperger, U., Furger, M., Gäggeler, H. W., Jost, D. T., Schwikowski, M., & Wanner, H. [1998]. Aerosol transport to the high Alpine sites Jungfraujoch [3454 m asl] and Colle Gnifetti [4452 m asl]. *Tellus B*, *50*[1], 76-92.

Luongo, M. T., Kurbatov, A. V., Erhardt, T., Mayewski, P. A., McCormick, M., More, A. F., ... & Bohleber, P. D. (2017). Possible Icelandic Tephra Found in European Colle Gnifetti Glacier. Geochemistry, geophysics, geosystems, 18(11), 3904-3909.

Luterbacher, J., Werner, J. P., Smerdon, J. E., Fernández-Donado, L., González-Rouco, F. J., Barriopedro, D., ... & Esper, J. [2016]. European summer temperatures since Roman times. Environmental Research Letters, 11[2], 024001.

Lüthi, M., & Funk, M. [2000]. Dating ice cores from a high Alpine glacier with a flow model for cold firn. Annals of Glaciology, 31, 69-79.

Ma, H., Chen, H., Gray, L., Zhou, L., Li, X., Wang, R., & Zhu, S. [2018]. Changing response of the North Atlantic/European winter climate to the 11 year solar cycle. Environmental Research Letters, 13[3], 034007.

Maasch, K. A., Mayewski, P. A., Rohling, E. J., Stager, J. C., Karlen, W., Meeker, L. D., & Meyerson, E. A. [2005]. A 2000-year context for modern climate change. Geografiska Annaler: Series A, Physical Geography, 87[1], 7-15.

Magnusdottir, G., Deser, C., & Saravanan, R. [2004]. The effects of North Atlantic SST and sea ice anomalies on the winter circulation in CCM3. Part I: Main features and storm track characteristics of the response. Journal of Climate, 17[5], 857-876.

Mann, M. E., & Jones, P. D. [2003]. Global surface temperatures over the past two millennia. Geophysical Research Letters, 30[15].

Mann, M. E., Zhang, Z., Hughes, M. K., Bradley, R. S., Miller, S. K., Rutherford, S., & Ni, F. [2008]. Proxy-based reconstructions of hemispheric and global surface temperature variations over the past two millennia. Proceedings of the National Academy of Sciences, 105[36], 13252-13257.

Mann, M. E., Zhang, Z., Rutherford, S., Bradley, R. S., Hughes, M. K., Shindell, D., ... & Ni, F. [2009]. Global signatures and dynamical origins of the Little Ice Age and Medieval Climate Anomaly. Science, 326[5957], 1256-1260.

Manning, J. G., Ludlow, F., Stine, A. R., Boos, W. R., Sigl, M., & Marlon, J. R. [2017]. Volcanic suppression of Nile summer flooding triggers revolt and constrains interstate conflict in ancient Egypt. Nature communications, 8[1], 900.

Maupetit, F., & Delmas, R. J. [1994]. Snow chemistry of high altitude glaciers in the French Alps. Tellus B: Chemical and Physical Meteorology, 46[4], 304-324.

Mayewski, P. A., Rohling, E. E., Stager, J. C., Karlén, W., Maasch, K. A., Meeker, L. D., ... & Lee-Thorp, J. [2004]. Holocene climate variability. Quaternary research, 62[3], 243-255.

Mayewski, P.A., Sneed, S.B., Birkel, S.D., Kurbatov, A.V. and Maasch, [2013]. Holocene warming marked by longer summers and reduced storm frequency around Greenland, Journal of Quaternary Science, 267-8179. DOI: 10.1002/jqs.2684.

Meeker, L. D., & Mayewski, P. A. [2002]. A 1400-year high-resolution record of atmospheric circulation over the North Atlantic and Asia. The Holocene, 12[3], 257-266.

Meola, M., Lazzaro, A., & Zeyer, J. [2015]. Bacterial composition and survival on Sahara dust particles transported to the European Alps. *Frontiers in microbiology*, *6*, 1454.

Middleton, N. J. [1985]. Effect of drought on dust production in the Sahel. *Nature*, *316*[6027], 431.

Miettinen, A., Divine, D. V., Husum, K., Koç, N., & Jennings, A. [2015]. Exceptional ocean surface conditions on the SE Greenland shelf during the Medieval Climate Anomaly. Paleoceanography, 30[12], 1657-1674.

Moberg, A., Sonechkin, D. M., Holmgren, K., Datsenko, N. M., & Karlén, W. [2005]. Highly variable Northern Hemisphere temperatures reconstructed from low-and high-resolution proxy data. Nature, 433[7026], 613.

More, A. F., Spaulding, N. E., Bohleber, P., Handley, M. J., Hoffmann, H., Korotkikh, E. V., ... & Mayewski, P. A. [2017]. Next-generation ice core technology reveals true minimum natural levels of lead [Pb] in the atmosphere: Insights from the Black Death. *GeoHealth*, *1*[4], 211-219

More, A. F., Spaulding, N. E., Bohleber, P., Handley, M. J., Hoffmann, H., Korotkikh, E. V., ... & Mayewski, P. A. [2018]. The Role of Historical Context in Understanding Past Climate, Pollution and Health Data in Trans-disciplinary Studies: Reply to Comments on More et al., 2017. GeoHealth, 2[5], 162-170.

Moreno, A., Pérez, A., Frigola, J., Nieto-Moreno, V., Rodrigo-Gámiz, M., Martrat, B., ... & Belmonte, Á. [2012]. The Medieval Climate Anomaly in the Iberian Peninsula reconstructed from marine and lake records. Quaternary Science Reviews, 43, 16-32.

Moulin, C., Lambert, C. E., Dulac, F., & Dayan, U. [1997]. Control of atmospheric export of dust from North Africa by the North Atlantic Oscillation. Nature, 387[6634], 691.

Moy, C. M., Seltzer, G. O., Rodbell, D. T., & Anderson, D. M. [2002]. Variability of El Niño/Southern Oscillation activity at millennial timescales during the Holocene epoch. Nature, 420[6912], 162.

Mulitza, S., Heslop, D., Pittauerova, D., Fischer, H. W., Meyer, I., Stuut, J. B., ... & Schulz, M. [2010]. Increase in African dust flux at the onset of commercial agriculture in the Sahel region. *Nature*, *466*[7303], 226.

Olsen, J., Anderson, N. J., & Knudsen, M. F. [2012]. Variability of the North Atlantic Oscillation over the past 5,200 years. Nature Geoscience, 5[11], 808.

Oman, L., Robock, A., Stenchikov, G. L., Thordarson, T., Koch, D., Shindell, D. T., & Gao, C. [2006]. Modeling the distribution of the volcanic aerosol cloud from the 1783–1784 Laki eruption. Journal of Geophysical Research: Atmospheres, 111[D12].

Oppenheimer, C., Orchard, A., Stoffel, M., Newfield, T. P., Guillet, S., Corona, C., ... & Büntgen, U. [2018]. The Eldgjá eruption: timing, long-range impacts and influence on the Christianisation of Iceland. *Climatic change*, *147*[3-4], 369-381.

Otterå, O. H., Bentsen, M., Drange, H., & Suo, L. [2010]. External forcing as a metronome for Atlantic multidecadal variability. Nature Geoscience, 3[10], 688.

Özsoy, E., Kubilay, N., Nickovic, S., & Moulin, C. [2001]. A hemispheric dust storm affecting the Atlantic and Mediterranean in April 1994: Analyses, modeling, ground-based measurements and satellite observations. Journal of Geophysical Research: Atmospheres, 106[D16], 18439-18460.

Pausata, F. S., Chafik, L., Caballero, R., & Battisti, D. S. [2015]. Impacts of high-latitude volcanic eruptions on ENSO and AMOC. Proceedings of the National Academy of Sciences, 112[45], 13784-13788.

Pederson, N., Hessl, A. E., Baatarbileg, N., Anchukaitis, K. J., & Di Cosmo, N. [2014]. Pluvials, droughts, the Mongol Empire, and modern Mongolia. Proceedings of the National Academy of Sciences, 111[12], 4375-4379.

Preunkert, S., Wagenbach, D., Legrand, M., & Vincent, C. [2000]. Col du Dôme [Mt Blanc Massif, French Alps] suitability for ice-core studies in relation with past atmospheric chemistry over Europe. Tellus B: Chemical and Physical Meteorology, 52[3], 993-1012.

Prospero, J. M. [1996]. Saharan dust transport over the North Atlantic Ocean and Mediterranean: An overview. In *The impact of desert dust across the Mediterranean* [pp. 133-151]. Springer, Dordrecht.

Prospero, J. M., & Lamb, P. J. [2003]. African droughts and dust transport to the Caribbean: Climate change implications. Science, 302[5647], 1024-1027.

Prospero, J. M., & Nees, R. T. [1986]. Impact of the North African drought and El Nino on mineral dust in the Barbados trade winds. Nature, 320[6064], 735.

Prospero, J. M., Blades, E., Mathison, G., and Naidu, R. [2005]. Interhemispheric transport of viable fungi and bacteria from Africa to the Caribbean with soil dust. Aerobiologia 21, 1–19. doi: 10.1007/s10453-004-5872-7

Prospero, J. M., Mayol-Bracero, O. L. [2013]. Understanding the Transport and Impact of African Dust on the Caribbean Basin. Bulletin of the American Meteorological Society, September 2013: 1329-1337.

Prospero, J. M., Schmitt, R., Cuevas, E., Savoie, D. L., Graustein, W. C., Turekian, K. K., ... & Levy, H. [1995]. Temporal variability of summer-time ozone and aerosols in the free troposphere over the eastern North Atlantic. Geophysical Research Letters, 22[21], 2925-2928.

Rein, B., Lückge, A., & Sirocko, F. [2004]. A major Holocene ENSO anomaly during the Medieval period. Geophysical Research Letters, 31[17].

Renssen, H., Goosse, H., & Muscheler, R. [2006]. Coupled climate model simulation of Holocene cooling events: oceanic feedback amplifies solar forcing. Climate of the Past, 2[2], 79-90.

Rodríguez, S., Cuevas, E., Prospero, J. M., Alastuey, A., Querol, X., López-Solano, J., ... & Alonso-Pérez, S. [2015]. Modulation of Saharan dust export by the North African dipole. Atmospheric Chemistry and Physics, 15[13], 7471-7486.

Schotterer, U., Oeschger, H., Wagenbach, D., & Münnich, K. O. [1985]. Information on paleo-precipitation on a high-altitude glacier Monte Rosa, Switzerland. *Zeitschrift für Gletscherkunde und Glazialgeologie*, *21*[1-2], 379-388.

Schwerzmann, A., Funk, M., Blatter, H., Lüthi, M., Schwikowski, M., & Palmer, A. [2006]. A method to reconstruct past accumulation rates in alpine firn regions: A study on Fiescherhorn, Swiss Alps. Journal of Geophysical Research: Earth Surface, 111[F1].

Schwikowski, M., Barbante, C., Doering, T., Gaeggeler, H. W., Boutron, C., Schotterer, U., ... & Rosman, K. [2004]. Post-17th-century changes of European lead emissions recorded in high-altitude alpine snow and ice. Environmental science & technology, 38[4], 957-964.

Schwikowski, M., Brütsch, S., Gäggeler, H. W., & Schotterer, U. [1999]. A high-resolution air chemistry record from an Alpine ice core: Fiescherhorn glacier, Swiss Alps. Journal of Geophysical Research: Atmospheres, 104[D11], 13709-13719.

Schwikowski, M., Seibert, P., Baltensperger, U., & Gaggeler, H. W. [1995]. A study of an outstanding Saharan dust event at the high-alpine site Jungfraujoch, Switzerland. Atmospheric Environment, 29[15], 1829-1842.

Shanahan, T. M., Overpeck, J. T., Anchukaitis, K. J., Beck, J. W., Cole, J. E., Dettman, D. L., ... & King, J. W. [2009]. Atlantic forcing of persistent drought in West Africa. science, 324[5925], 377-380.

Shindell, D. T., Schmidt, G. A., Mann, M. E., Rind, D., & Waple, A. [2001]. Solar forcing of regional climate change during the Maunder Minimum. Science, 294[5549], 2149-2152.

Shindell, D. T., Schmidt, G. A., Miller, R. L., & Mann, M. E. [2003]. Volcanic and solar forcing of climate change during the preindustrial era. Journal of Climate, 16[24], 4094-4107.

Sigl, M., Winstrup, M., McConnell, J. R., Welten, K. C., Plunkett, G., Ludlow, F., ... & Fischer, H. [2015]. Timing and climate forcing of volcanic eruptions for the past 2,500 years. Nature, 523[7562], 543.

Skonieczny, C., McGee, D., Winckler, G., Bory, A., Bradtmiller, L. I., Kinsley, C. W., ... & Malaizé, B. [2019]. Monsoon-driven Saharan dust variability over the past 240,000 years. Science advances, 5[1], eaav1887.

Sneed, Sharon B., et al. [2015]. "New LA-ICP-MS cryocell and calibration technique for sub-millimeter analysis of ice cores." Journal of glaciology 61, no. 226, 233-242.\

Sodemann, H., Palmer, A. S., Schwierz, C., Schwikowski, M., & Wernli, H. [2006]. The transport history of two Saharan dust events archived in an Alpine ice core. Atmospheric Chemistry and Physics, 6[3], 667-688.

Spaulding, Nicole E., et al. "A New Multielement Method for LA-ICP-MS Data Acquisition from Glacier Ice Cores." Environmental science & technology 51, no. 22 [2017]: 13282-13287.

Steinhilber, F., Abreu, J. A., Beer, J., Brunner, I., Christl, M., Fischer, H., ... & Miller, H. [2012]. 9,400 years of cosmic radiation and solar activity from ice cores and tree rings. Proceedings of the National Academy of Sciences, 109[16], 5967-5971.

Steinhilber, F., Beer, J., & Fröhlich, C. [2009]. Total solar irradiance during the Holocene. Geophysical Research Letters, 36[19].

Thevenon, F., Anselmetti, F. S., Bernasconi, S. M., & Schwikowski, M. [2009]. Mineral dust and elemental black carbon records from an Alpine ice core [Colle Gnifetti glacier] over the last millennium. Journal of Geophysical Research: Atmospheres, 114[D17].

Thevenon, F., Chiaradia, M., Adatte, T., Hueglin, C., & Poté, J. [2011]. Ancient versus modern mineral dust transported to high-altitude Alpine glaciers evidences Saharan sources and atmospheric circulation changes. *Atmospheric Chemistry and Physics Discussions*, [1], 859-884.

Thompson, L. G., Yao, T., Mosley-Thompson, E., Davis, M. E., Henderson, K. A., & Lin, P. N. [2000]. A high-resolution millennial record of the South Asian monsoon from Himalayan ice cores. Science, 289[5486], 1916-1919.

Thordarson, T., & Self, S. [2003]. Atmospheric and environmental effects of the 1783–1784 Laki eruption: A review and reassessment. Journal of Geophysical Research: Atmospheres, 108[D1].

Trouet, V., Esper, J., Graham, N. E., Baker, A., Scourse, J. D., & Frank, D. C. [2009]. Persistent positive North Atlantic Oscillation mode dominated the medieval climate anomaly. science, 324[5923], 78-80.

Varga, G., Kovács, J., & Újvári, G. [2013]. Analysis of Saharan dust intrusions into the Carpathian Basin [Central Europe] over the period of 1979–2011. Global and Planetary Change, 100, 333-342.

W. C. Jordan. [2010]. "The Great Famine Revisited" in Scott Bruce ed., Ecologies and Economies in Medieval and Early Modern Europe: Studies in Environmental History for Richard C. Hoffmann [Leiden: Brill], 45-62, at 53.

W. C. Jordan. [1996]. The Great Famine:Northern Europe in the Early Fourteenth Century, [Princeton: Princeton University Press], 142-48, 185-6.

Wagenbach, D., & Geis, K. [1989]. The mineral dust record in a high altitude Alpine glacier [Colle Gnifetti, Swiss Alps]. In Paleoclimatology and paleometeorology: modern and past patterns of global atmospheric transport [pp. 543-564]. Springer, Dordrecht.

Wagenbach, D., Bohleber, P., & Preunkert, S. [2012]. Cold, alpine ice bodies revisited: what may we learn from their impurity and isotope content?. Geografiska Annaler: Series A, Physical Geography, 94[2], 245-263.

Wang, C., Dong, S., Evan, A. T., Foltz, G. R., & Lee, S. K. [2012]. Multidecadal covariability of North Atlantic sea surface temperature, African dust, Sahel rainfall, and Atlantic hurricanes. Journal of Climate, 25[15], 5404-5415.

Wassenburg, J. A., Immenhauser, A., Richter, D. K., Niedermayr, A., Riechelmann, S., Fietzke, J., ... & Sabaoui, A. [2013]. Moroccan speleothem and tree ring records suggest a variable positive state of the North Atlantic Oscillation during the Medieval Warm Period. Earth and Planetary Science Letters, 375, 291-302.

Weikinn, C. [2002]. Quellentexte zur Witterungsgeschicte Europas von der Zeitwende bis zum Jahr 1850. Berlin: Gebrüder Borntraeger.

Wheeler, D. [1985]. Saharan dust storm over England.

Wheeler, D. A. [1986]. The meteorological background to the fall of Saharan dust, November 1984. Meteorological Magazine, 115[1362], 1-9.

White, Lynn Townsend. [1962]. *Medieval technology and social change*. Oxford: Clarendon Press.

Williamson, Tom. [2013]. *Environment, society and landscape in early medieval England: time and topography*. 1st ed. Woodbridge, Suffolk, UK; Rochester, NY: Boydell Press.

Xoplaki, E., Fleitmann, D., Diaz, H., von Gunten, L., & Kiefer, T. (2011). Medieval climate anomaly. *PAGES news*, *19*(1), 1-32.

Zhu, X. R., Prospero, J. M., & Millero, F. J. [1997]. Diel variability of soluble Fe [II] and soluble total Fe in North African dust in the trade winds at Barbados. Journal of Geophysical Research: Atmospheres, 102[D17], 21297-21305.
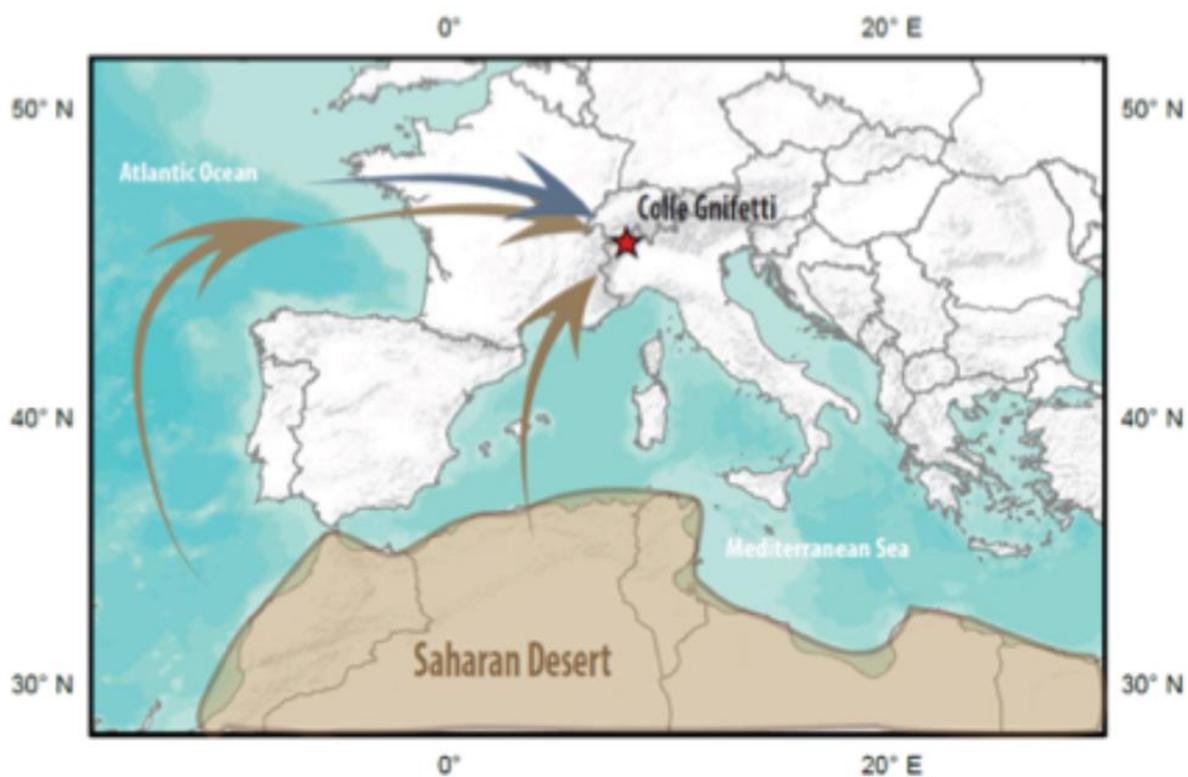
Figure 1 Summer trajectories for Saharan dust to Colle Gnifetti. Idealized modern summer trajectories for Saharan dust from Hysplit back-trajectories in Schwikowski, et al. (1995) and Thevenon et al. (2012) (brown arrow) and marine airmass transport (blue arrow) to Colle Gnifetti ice core site (red star).
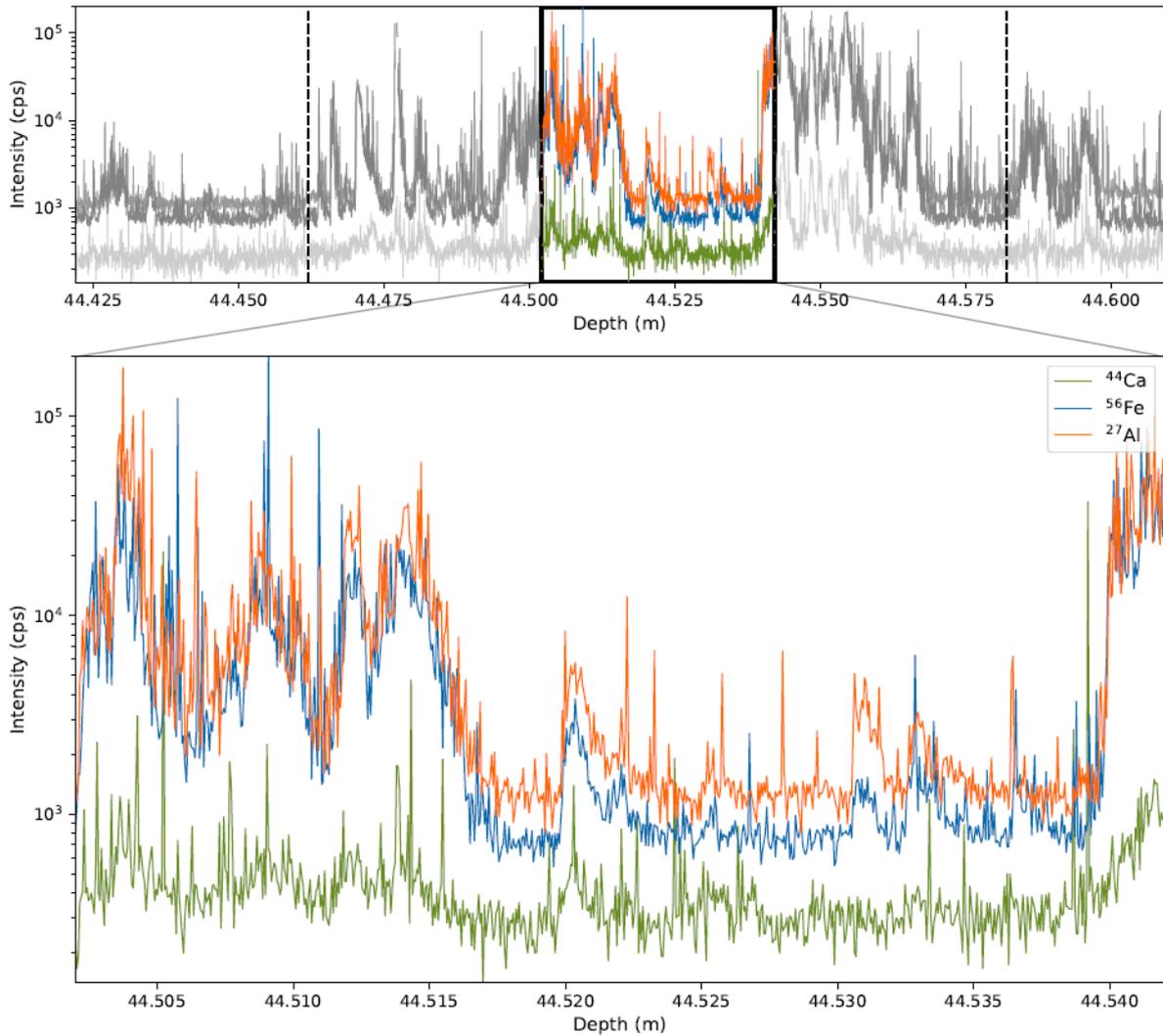
Figure 2 Example of LA-ICP-MS 4-cm runs. a. Example of ^{56}Fe (blue), ^{27}Al (orange), ^{44}Ca (green) in intensity as counts per second (cps) collected simultaneously, pre-processed and concatenated for a section (~18-cm) of the CG ice core, highlighted area shows the 4-cm run from B. **b.** Example of ^{56}Fe (blue), ^{27}Al (orange), ^{44}Ca (green) in intensity as counts per second (cps) collected simultaneously during a 4-cm run.
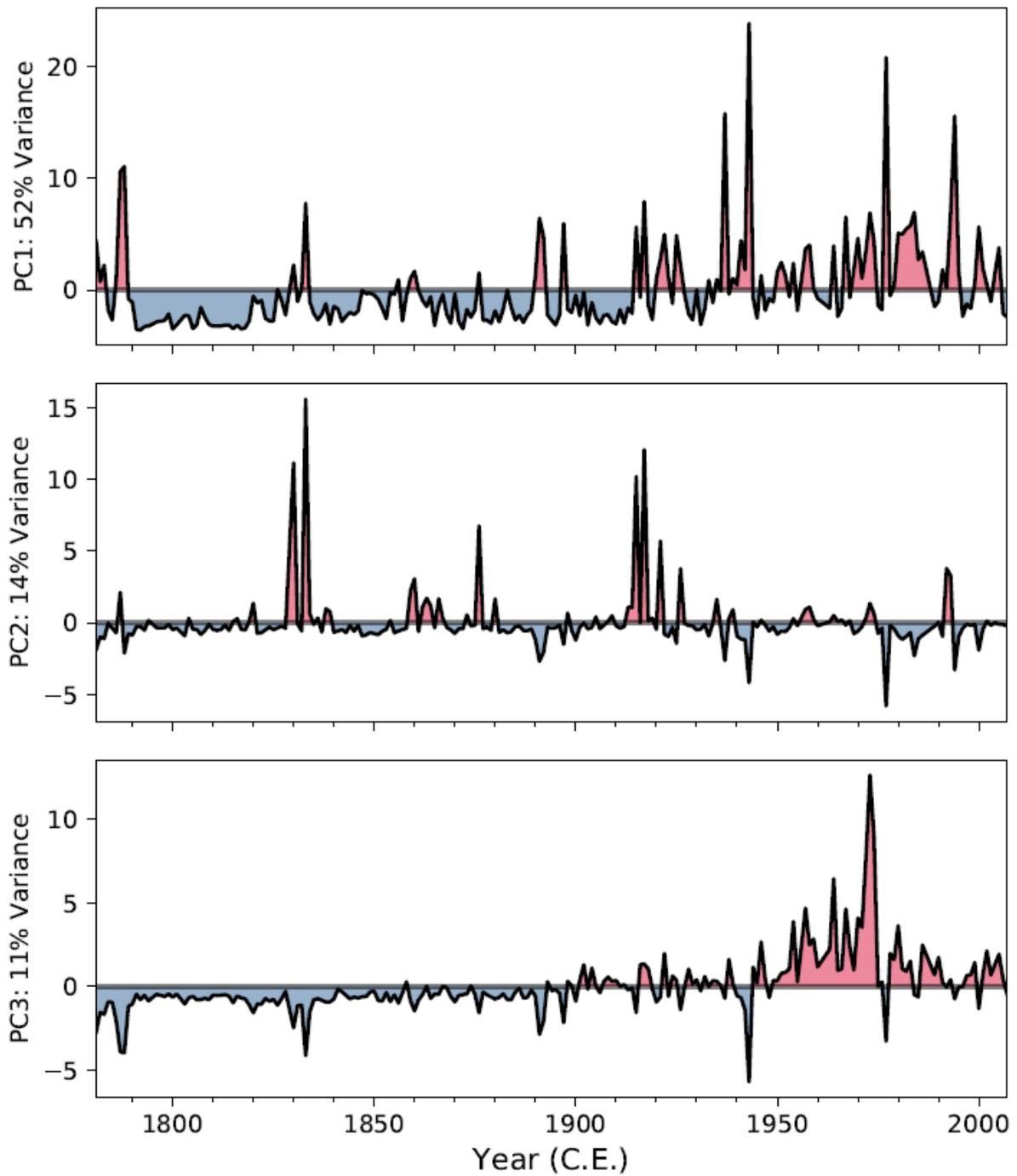
Figure 3 PCA Results. The three dominant principal components from principal component analysis resulting from annually resampled ICP-MS data of 26 major and trace elements and 3 anions from IC data, for the period 1780-2006 generated using sci-kit in Python.
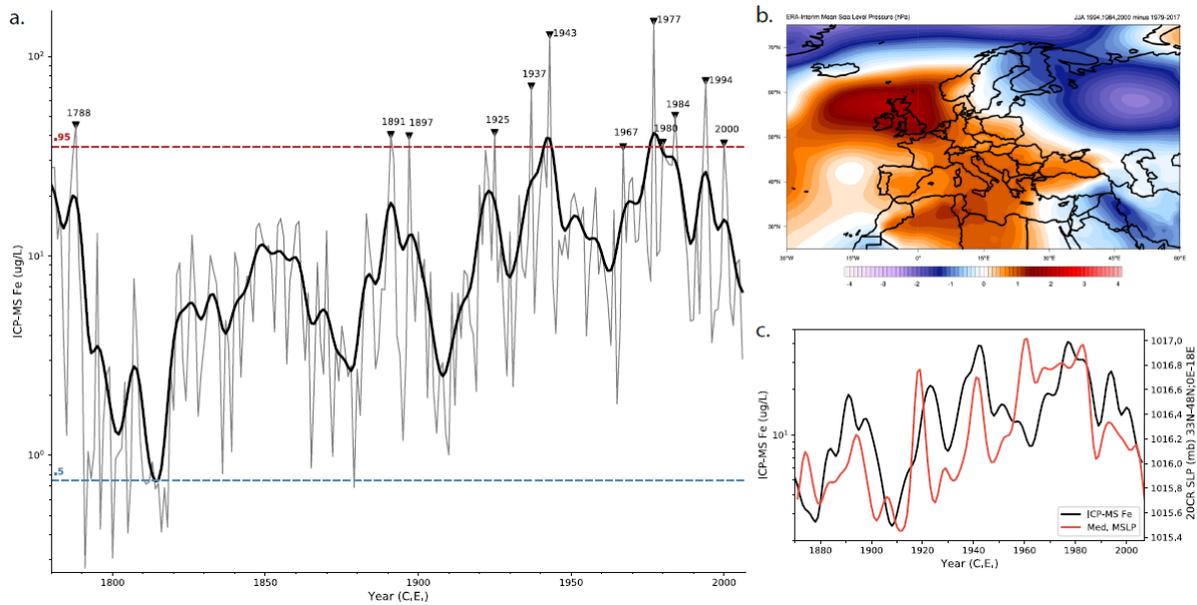
Figure 4 Saharan dust proxy 1780-2006. a. Annual smooth Saharan dust proxy (black) for 1780-2006, derived from annual mean ICP-MS Fe (black), shown in log scale to allow a view of the full concentration variability. Black triangles show years with concentrations > 0.95 percentile, discussed in Table S3. **b.** Top 3 SDE years (1984, 1994, 2000) post 1979 from compiled ERA-Interim Reanalysis data for MSLP during JJA. **c**. Comparison of CR20 v2 MSLP (red) smoothed from the Mediterranean region (33N-48N;0E-18E) to annual smooth ICP-MS Fe (black) for 1870-2007, with a statistically significant R-value of 0.66.
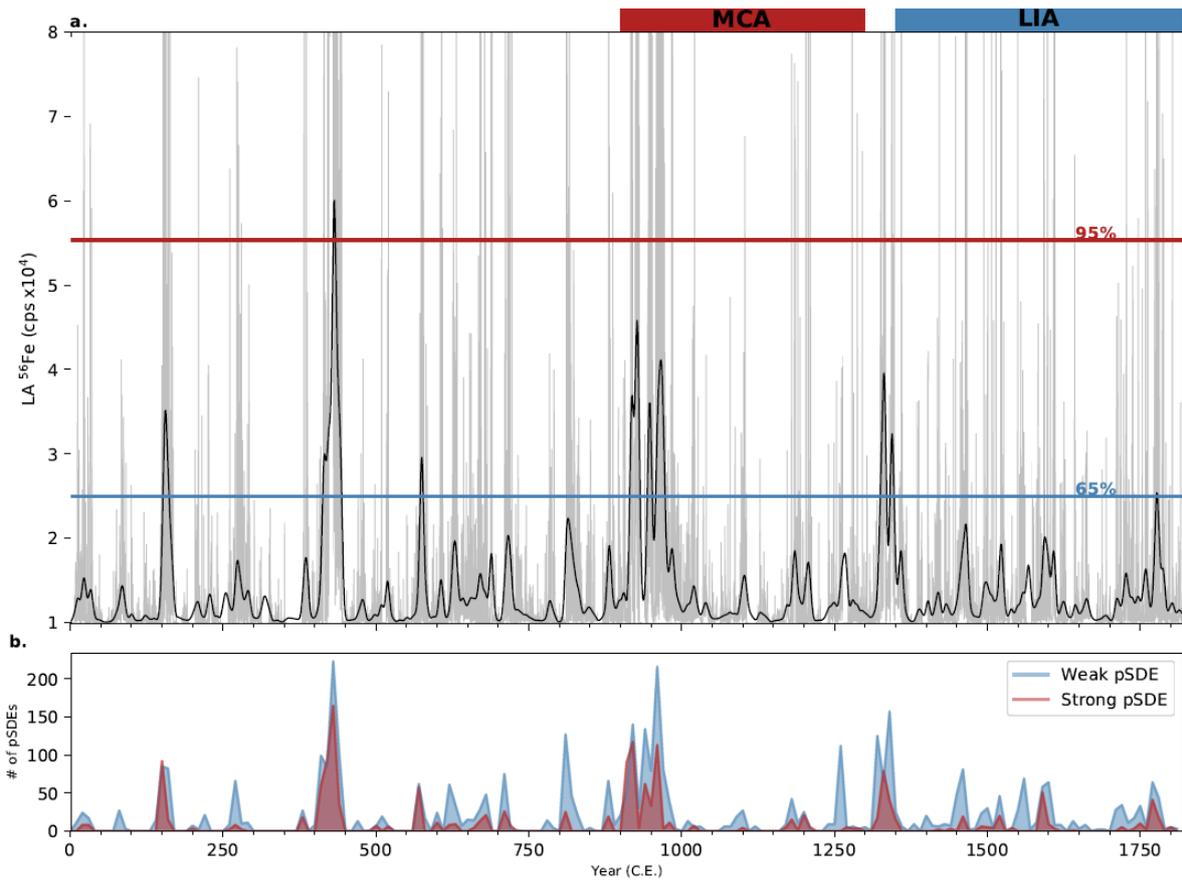
Figure 5 Saharan Dust Event Proxy 1-1820 C.E. a. pSDE record shown with 0.02-year (grey) and smoothed annually resampled LA-ICP-MS ⁵⁶Fe (black) b. Number of strong (red) and weak (blue) pSDEs, binned by decade, overlapped. MCA (Medieval Climate Anomaly) and LIA (Little Ice Age) time periods shown above plot.
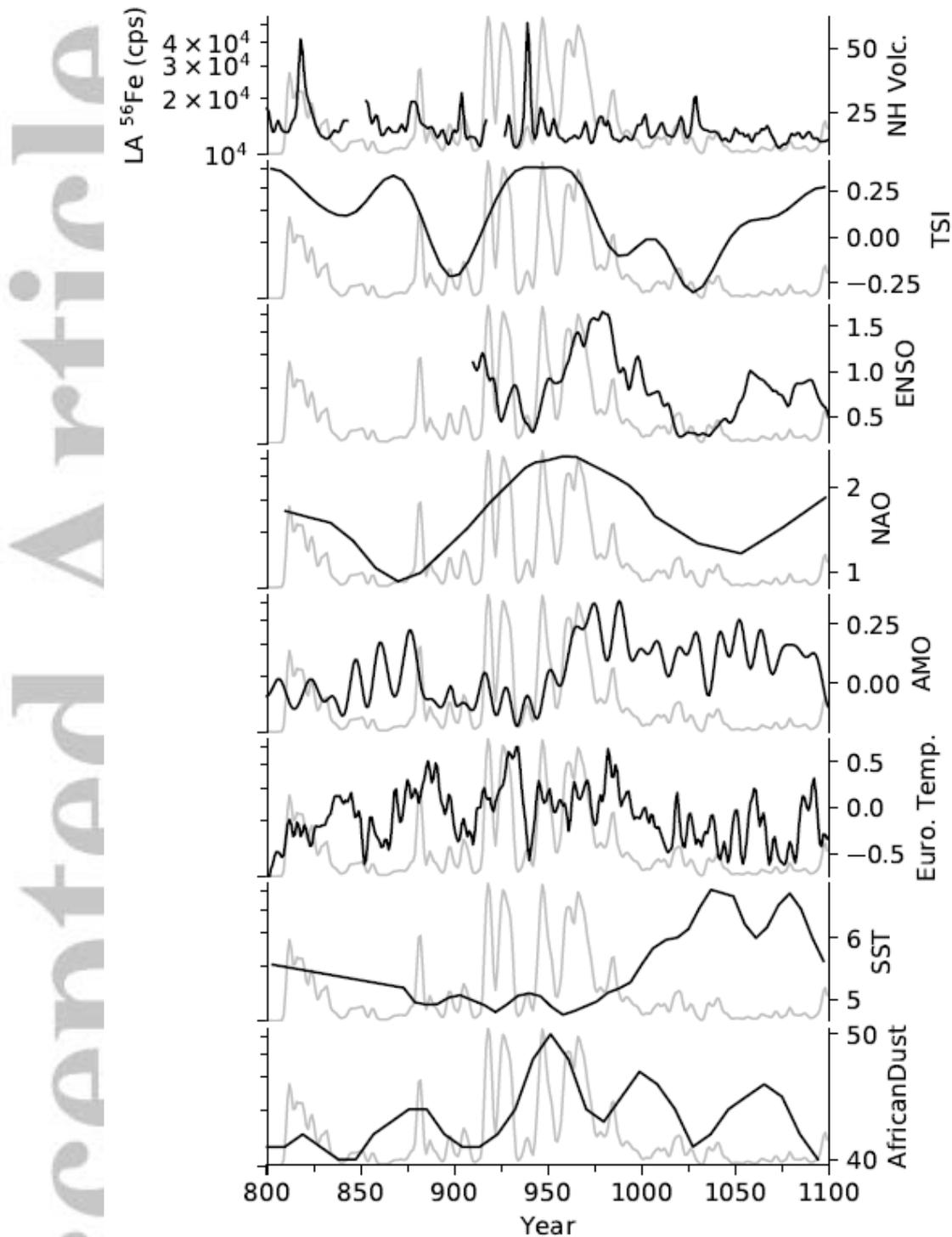
Figure 6 Onset of Medieval Climate Anomaly Proxy Comparison. Common Era climate forcings /ocean-atmospheric teleconnection proxy comparison with a) NH volcanic events (Sigl et al., 2015), total solar irradiance (Steinhilber et al., 2009), reconstructed ENSO record (Li et al., 2011), NAO index (Trouet et al., 2009) and extended reconstructed NAO index (Olsen et al., 2012), reconstructed AMO index (Mann et al., 2009), and reconstructed European JJA temperature (Luterbacher et al., 2016), North Atlantic SST (Miettinen et al., 2015), and dust deposition record from northwest Africa, based on a marine-derived grain-size distribution of terrigenous sediments (>10 μm; Mulitza et al., 2010) compared to smoothed LA-ICP-MS annual resolution ^{56}Fe data from this study (grey).
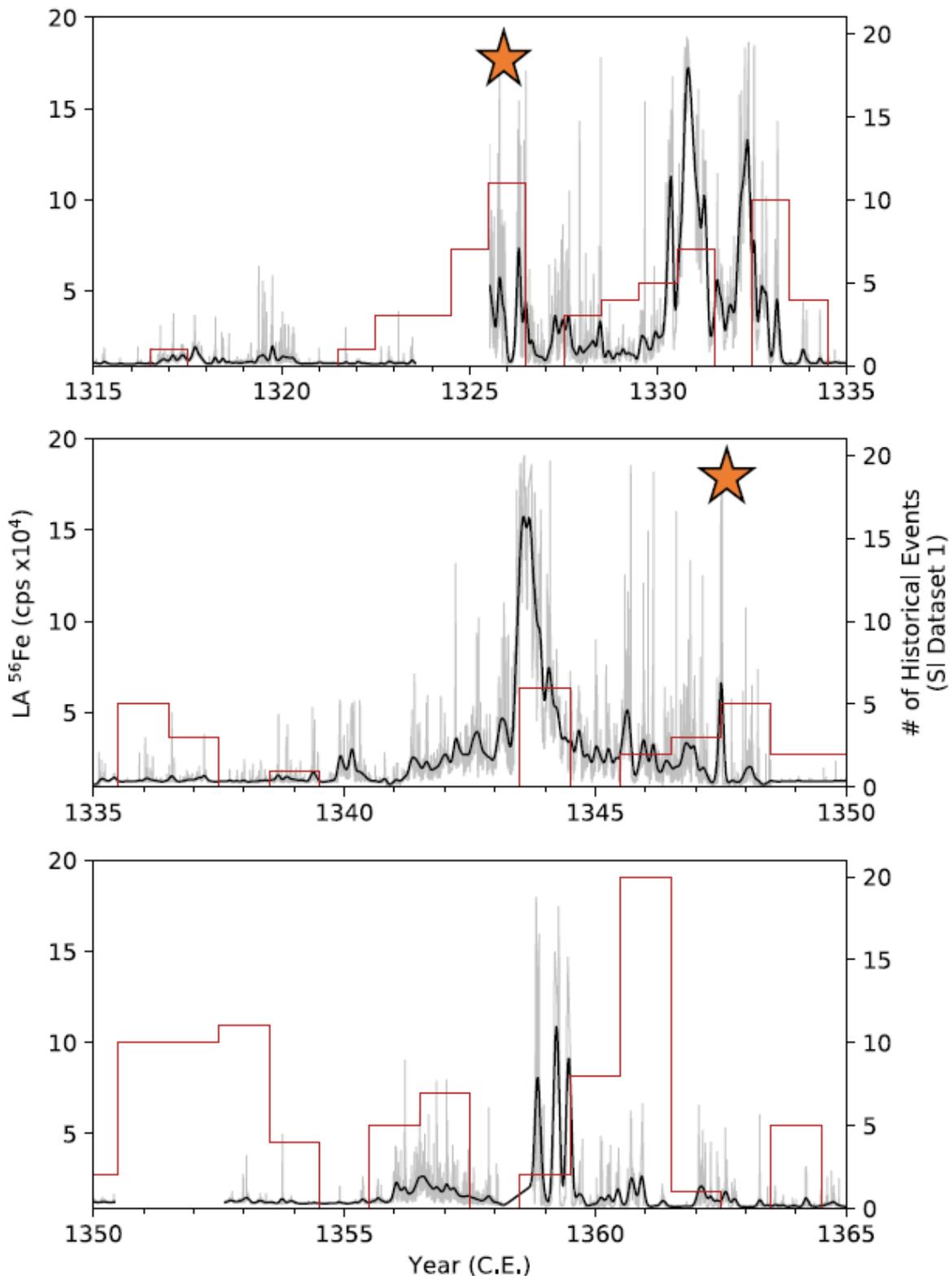
Figure 7 Anomalous SDEs in the mid-1300s. Outstanding Saharan dust episodes at Colle Gnifetti in the pre-instrumental period, found in both the Fe and ^{56}Fe records (1315-1365) shown with raw (grey) and smoothed (black) ^{56}Fe intensity (120-μm). Number of historical events that account for drought and heat events in Europe shown in red shown with right axis. Orange stars signify historical records of dust events.